cases of PEEK-*g*-PMPC with/without BP, an approximately 100-nm-thick PMPC layer was clearly observed on the surface of the PEEK substrate, and neither crack nor delamination was observed at the PEEK substrate and the interface between the PMPC layer and the PEEK substrate. These results indicate that the PMPC layer formed on the PEEK substrate is uniformly distributed over the substrate and is bound to the substrate by covalent C−C bonds. Because the photoinduced radical graft polymerization proceeds only on the surface of the PEEK substrate, the properties of the substrate remain unchanged. Retention of the properties of the PEEK substrate is very important in clinical use because the biomaterials used in implants act not only as functional materials but also as structural materials in vivo. During the polymerization of PEEK-*g*-PMPC with BP, the pinacolization reaction was photoinduced (UV irradiation) not only by the BP unit in PEEK but also by the BP initiators precoated on the substrate. However, the amount of semibenzopinacol radicals produced from the BP units in PEEK alone would be sufficient to induce surface-initiated graft polymerization, since there is no clear difference in the PMPC layer between the PEEK-*g*-PMPC with and without BP.

Table 1 summarizes the static water-contact angles and the amount of BSA adsorbed on the untreated PEEK and PEEK-*g*-PMPC with/without BP. The static water-contact angle of the untreated PEEK was 92.5°, and it decreased markedly to 7.1° ($p < 0.001$) and 6.8° ($p < 0.001$), respectively, after PMPC grafting was carried out with/without BP. Because MPC is a highly hydrophilic compound, PMPC is water-soluble (8−12). The water wettability of the PEEK-*g*-PMPC surface was considerably greater than that of the untreated PEEK surface because of the presence of a PMPC nanometer-scale layer (Figure 4). The fluid (water) film forming ability of the PEEK-*g*-PMPC surface can be attributed to such a nanometer-scale thin PMPC layer because the outermost PMPC layer determines this ability. The adsorption of the representative plasma protein and BSA on the PEEK-*g*-PMPC surface considerably decreased to 20% ($p < 0.001$) compared to that in the case of the untreated PEEK (0.08 $\mu g/cm^2$). It is hypothesized that the mechanism of protein adsorption resistance on the surface modified by the MPC polymer is attributed to the water structure resulting from the interactions between the water molecules and phosphorylcholine groups (27−30). The presence of a large amount of free water around the phosphorylcholine group is responsible for the easy detachment of proteins and the prevention of conformational changes in the adsorbed proteins (29). A decrease in protein adsorption is also considered to be caused by the presence of a hydrated layer around the phosphorylcholine groups (27). These observations are consistent with the results of the static water-contact angle measurements and cross-sectional TEM observations of the PEEK whose surface is modified by PMPC grafting. These results imply that the PEEK-*g*-PMPC surface is biocompatible in terms of tissue and blood compatibility because MPC polymer modified surfaces are known to exhibit in vivo biocompatibility (8−14).

The novel and simple photoinduced graft polymerization in the absence of photoinitiators would be highly suitable for industrial applications (31, 32) as well as the development of medical devices (2−7). The density and thickness of the grafting layer can be controlled by the photoirradiation time and monomer concentration (16, 17). Additional efforts are needed in this aspect. However, the synthesis of a self-initiated biocompatible polymer having unique properties such as antiprotein adsorption and wettability by the photoinduced "grafting-from" polymerization reaction is indeed a novel and simple phenomenon developed in the field of biomaterials science, and the fabrication of the PEEK-*g*-PMPC surface can result in the development of next-generation multifunctional biomaterials.

CONCLUSION

A biocompatible and highly hydrophilic nanometer-scale modified surface was successfully fabricated on the PEEK substrate by the photoinduced graft polymerization of PMPC in the absence of photoinitiators. Because MPC is a highly hydrophilic compound, the water wettability of the PEEK-*g*-PMPC surface was greater than that of the untreated PEEK surface because of the formation of a PMPC nanometer-scale layer. In addition, the amount of BSA adsorbed on the PEEK-*g*-PMPC surface considerably decreased compared to that in the case of untreated PEEK. This novel and simple photoinduced graft polymerization in the absence of photoinitiators is highly suitable in industrial applications, including the development of medical devices.

REFERENCES AND NOTES

(1) Brown, S. A.; Hastings, R. S.; Mason, J. J.; Moet, A. *Biomaterials* **1990**, *11*, 541–547.
(2) Kurtz, S. M.; Devine, J. N. *Biomaterials* **2007**, *28*, 4845–4869.
(3) Wang, A.; Lin, R.; Stark, C.; Dumbleton, J. H. *Wear* **1999**, 225–229, and 724–727.
(4) Joyce, T. J.; Rieker, C.; Unsworth, A. *Biomed. Mater. Eng.* **2006**, *16*, 1–10.
(5) Latif, A. M. H.; Mehats, A.; Elcocks, M.; Rushton, N.; Field, R. E.; Jones, E. *J. Mater. Sci. Mater. Med.* **2008**, *19*, 1729–1736.
(6) Yu, S.; Hariram, K. P.; Kumar, R.; Cheang, P.; Aik Khor, K. *Biomaterials* **2005**, *26*, 2343–2352.
(7) Fan, J. P.; Tsui, C. P.; Tang, C. Y.; Chow, C. L. *Biomaterials* **2004**, *25*, 5363–5373.
(8) Ishihara, K.; Ueda, T.; Nakabayashi, N. *Polym. J.* **1990**, *22*, 355–360.
(9) Ishihara, K.; Iwasaki, Y.; Ebihara, S.; Shindo, Y.; Nakabayashi, N. *Colloids Surf. B* **2000**, *18*, 325–335.
(10) Kyomoto, M.; Iwasaki, Y.; Moro, T.; Konno, T.; Miyaji, F.; Kawaguchi, H.; Takatori, Y.; Nakamura, K.; Ishihara, K. *Biomaterials* **2007**, *28*, 3121–3130.
(11) Ueda, H.; Watanabe, J.; Konno, T.; Takai, M.; Saito, A.; Ishihara, K. *J. Biomed. Mater. Res. A* **2006**, *77*, 19–27.
(12) Snyder, T. A.; Tsukui, H.; Kihara, S.; Akimoto, T.; Litwak, K. N.; Kameneva, M. V.; Yamazaki, K.; Wagner, W. R. *J. Biomed. Mater. Res. A* **2007**, *81*, 85–92.
(13) Moro, T.; Takatori, Y.; Ishihara, K.; Konno, T.; Takigawa, Y.; Matsushita, T.; Chung, U. I.; Nakamura, K.; Kawaguchi, H. *Nat. Mater.* **2004**, *3*, 829–837.
(14) Moro, T.; Takatori, Y.; Ishihara, K.; Nakamura, K.; Kawaguchi, H. *Clin. Orthop. Relat. Res.* **2006**, *453*, 58–63.
(15) Kyomoto, M.; Moro, T.; Konno, T.; Takadama, H.; Kawaguchi, H.; Takatori, Y.; Nakamura, K.; Yamawaki, N.; Ishihara, K. *J. Mater. Sci. Mater. Med.* **2007**, *18*, 1809–1815.
(16) Kyomoto, M.; Moro, T.; Konno, T.; Takadama, H.; Yamawaki, N.; Kawaguchi, H.; Takatori, Y.; Nakamura, K.; Ishihara, K. *J. Biomed. Mater. Res. A* **2007**, *82*, 10–17.

(17) Kyomoto, M.; Moro, T.; Miyaji, F.; Hashimoto, M.; Kawaguchi, H.; Takatori, Y.; Nakamura, K.; Ishihara, K. *J. Biomed. Mater. Res. A* **2008**, *86*, 439–447.
(18) Giancaterina, S.; Rossi, A.; Rivaton, A.; Gardette, J. L. *Polym. Degrad. Stab.* **2000**, *68*, 133–144.
(19) Wang, H.; Brown, H. R.; Li, Z. *Polymer* **2007**, *48*, 939–948.
(20) Yang, W.; Rånby, B. *Eur. Polym. J.* **1999**, *35*, 1557–1568.
(21) Qiu, C.; Nguyen, Q. T.; Ping, Z. *J. Membr. Sci.* **2007**, *295*, 88–94.
(22) Nguyen, H. X.; Ishida, H. *Polymer* **1986**, *27*, 1400–1405.
(23) Cole, K. C.; Casella, I. G. *Thermochim. Acta* **1992**, *211*, 209–228.
(24) Qiu, K. Y.; Si, K. *Macromol. Chem. Phys.* **1996**, *197*, 2403–2413.
(25) He, D.; Susanto, H.; Ulbricht, M. *Prog. Polym. Sci.* **2009**, *34*, 62–98.
(26) Deng, J.; Wang, L.; Liu, L.; Yang, W. *Prog. Polym. Sci.* **2009**, *34*, 156–193.
(27) Goda, T.; Konno, T.; Takai, M.; Ishihara, K. *Colloids Surf. B* **2007**, *54*, 67–73.
(28) Futamura, K.; Matsuno, R.; Konno, T.; Takai, M.; Ishihara, K. *Langmuir* **2008**, *24*, 10340–10344.
(29) Ishihara, K.; Nomura, H.; Mihara, T.; Kurita, K.; Iwasaki, Y.; Nakabayashi, N. *J. Biomed. Mater. Res.* **1998**, *39*, 323–330.
(30) Hoshi, T.; Sawaguchi, T.; Konno, T.; Takai, M.; Ishihara, K. *Polymer* **2007**, *48*, 1573–1580.
(31) Hasegawa, S.; Suzuki, Y.; Maekawa, Y. *Radiat. Phys. Chem.* **2008**, *77*, 617–621.
(32) Chen, J.; Asano, M.; Maekawa, Y.; Yoshida, M. *J. Membr. Sci.* **2008**, *319*, 1–4.

AM800260T

RAFT Synthesis and Stimulus-Induced Self-Assembly in Water of Copolymers Based on the Biocompatible Monomer 2-(Methacryloyloxy)ethyl Phosphorylcholine

Bing Yu,[†] Andrew B. Lowe,*[,‡] and Kazuhiko Ishihara[§]

Department of Chemistry and Biochemistry, and School of Polymers and High Performance Materials, University of Southern Mississippi, 118 College Drive, No. 10076, Hattiesburg, Mississippi 39406, and Department of Materials Engineering, School of Engineering, The University of Tokyo, 7-3-1, Hongo, Bunkyo-ku, Tokyo 113-8656, Japan

Received December 23, 2008

Reversible addition-fragmentation chain transfer (RAFT) radical polymerization, mediated by 4-cyanopentanoic acid dithiobenzoate and 4,4′-azobis(4-cyanovaleric acid) (V-501) in water at 70 °C, of biocompatible 2-(methacryloyloxy)ethyl phosphorylcholine (MPC) yields a macro-chain transfer agent (CTA) that was employed in the synthesis of a range of stimulus-responsive AB diblock copolymers in protic media. Well-defined block copolymers of varying molar composition, with narrow molecular weight distributions ($M_w/M_n = 1.10-1.24$) were prepared with *N*,*N*-diethylacrylamide (DEAm), 4-vinylbenzoic acid (VBZ), *N*-(3-sulfopropyl)-*N*-methacryloyloxyethyl-*N*,*N*-dimethylammonium betaine (DMAPS), and the newly synthesized *N*,*N*-di-*n*-propylbenzylvinylamine (Dn-PBVA) in either methanol, 2,2,2-trifluoroethanol, or aqueous media. When a combination of ^{1}H NMR spectroscopy and dynamic light scattering is used, it is shown that all block copolymers are capable of existing as molecularly dissolved chains in aqueous media with average hydrodynamic diameters of ~6−7 nm provided the aqueous environment is appropriately tuned. Similarly, these unimers can be induced to undergo self-assembly in the same aqueous environment provided the correct external stimulus (change in temperature, pH, or electrolyte concentration) is applied. In such instances, aggregates with average sizes in the range of ~22−180 nm are formed and are most likely due to the formation of polymeric micelles and vesicles. Such self-assembly is also completely reversible. Removal, or reversal, of the applied stimulus results in the reorganization to the unimeric state.

Introduction

Polymeric betaines (polybetaines) are zwitterionic materials in which the cationic and anionic functional groups are located on the same monomer/repeat unit.[1,2] Such materials may be further differentiated based on the chemical nature of the negatively charged group and include the sulfo- (sulfonate),[3,4] carboxy- (carboxylate),[5−9] and phospho- (phosphonate)[10−17] betaines, as well as the less well-known dicyanoetheneolates.[18−22] Polybetaines were first reported in the 1950s[23,24] and since then have almost exclusively been prepared via the direct homogeneous aqueous solution radical polymerization of the corresponding betaine monomer. The preparation of well-defined polybetaines, as well as materials with more advanced architectures, has only been accomplished relatively recently. Lowe et al.[25−29] reported the group transfer polymerization synthesis of poly(2-(dimethylamino)ethyl methacrylate) (PDMAEMA) homopolymers as well as copolymers with various methacrylic comonomers of controlled molecular weight and low polydispersity that were modified postpolymerization by reaction of the tertiary amine residues in the DMAEMA residues with 1,3-propanesultone yielding the corresponding well-defined polysulfopropylbetaines. Such polymer analogous reactions are facile, selective, and essentially quantitative. The advent of controlled radical polymerization techniques has facilitated the direct (co)polymerization of sulfo-, carboxy-, and phosphobetaine monomers. For example, atom transfer radical polymerization has been employed extensively by Armes and co-workers in the preparation of a wide-range of materials based on the methacrylic phosphobetaine monomer 2-(methacryloyloxy)ethyl phosphorylcholine (MPC).[13,30−32] MPC is especially interesting given its well-documented biocompatibility.[11,12,33−40] Most recently, the direct[41] and indirect[42] synthesis of well-defined polysulfo- and polycarboxybetaines was accomplished by ring-opening metathesis polymerization (ROMP). Rankin and Lowe[41] described the rapid, direct, controlled homo- and copolymerization of *exo*-7-oxanorbornene sulfo- and carboxybetaine derivatives employing a novel 2,2,2-trifluoroethanol/CH_2Cl_2 solvent combination in conjunction with Grubbs first generation catalyst $RuCl_2(PCy_3)_2CHPh$. The only requirement for successful (co)polymerization was that the carboxybetaine be polymerized in the free acid form to prevent competitive complexation of carboxylate functional groups to the Ru metal center. Colak and Tew[42] disclosed the synthesis of oxa- and methylene bridged norbornene-based polycarboxybetaines employing protecting group chemistry. Polymerizations of ammonium monomers with *tert*-butyl ester groups were performed in THF/methanol at 60 °C employing the third generation Grubbs catalyst $RuCl_2PCy_3(3\text{-}BrPy)_2CHPh$. The free carboxybetaines were obtained postpolymerization by treatment with neat trifluoroacetic acid.

Reversible addition-fragmentation chain transfer (RAFT) radical polymerization[43−47] is, arguably, the most versatile of

* To whom correspondence should be addressed. E-mail: andrew.lowe@usm.edu.
† Department of Chemistry and Biochemistry, University of Southern Mississippi.
‡ School of Polymers and High Performance Materials, University of Southern Mississippi.
§ Department of Materials Engineering, The University of Tokyo.

10.1021/bm8014945 CCC: $40.75
Published on Web 02/25/2009

Table 1

entry	block copolymer	M_n expt	M_p expt[f]	M_w/M_n[f]	theoretical molar composition[g]	measured molar composition[h]
1	P(MPC-*b*-DEAm)[a]	12400	12900	1.10	80:20	82:18
2	P(MPC-*b*-DEAm)[a]	10700	12500	1.24	50:50	56:44
3	P(MPC-*b*-VBZ)[b]	10400	11100	1.10	80:20	89:11
4	P(MPC-*b*-VBZ)[b]	10200	11800	1.16	50:50	50:50
5	P(MPC-*b*-DnPBVA)[c]	11000	11700	1.18	50:50	70:30
6	P(MPC-*b*-DMAPS)[d]	12000	13300	1.13	70:30	76:24
7	P(MPC-*b*-DMAPS)[e]	12000	13500	1.17	50:50	58:42

[a] Polymerization conducted at 60 °C with thiocarbonylthio end-group/V-501 = 3:1 at a concentration of 25 wt % in MeOH. [b] Polymerization conducted at 80 °C with thiocarbonylthio end-group/V-501 = 3:1 at a concentration of 10 wt % in deionized water with 1 mol equiv of Na_2CO_3 based on VBZ to aid in the dissolution of the styrenic monomer. [c] Polymerization conducted at 70 °C with thiocarbonylthio end-group/V-501 = 3:1 at a concentration of 10 wt % in 2,2,2-trifluoroethanol. [d] Polymerization conducted at 60 °C with thiocarbonylthio end-group/V-501 = 3:1 at a concentration of 25 wt % in methanol. [e] Polymerization conducted at 80 °C with thiocarbonylthio end-group/V-501 = 3:1 at a concentration of 10 wt % in 0.25 M NaBr. [f] As determined by aqueous size exclusion chromatography, in 0.25 M NaBr, calibrated with narrow molecular mass poly(ethylene oxide) standards. [g] Assuming 100% conversion of the second block. [h] As determined by ^{1}H NMR spectroscopy.

the controlled radical polymerization techniques facilitating the controlled polymerization of the broadest range of monomer families. For example, aside from the common monomer families such as styrenics,[48−53] (meth)acrylates,[54,55] and (meth)acrylamides,[51−53,56−61] RAFT is suitable for nonactivated substrates such as vinyl esters,[62] vinyl amides,[62,63] and diallylammonium species.[64] RAFT has also been employed in the (co)polymerization of betaine monomers. The first report highlighting the application of RAFT in the synthesis of polybetaines was that of Laschewsky et al.[65] and was shortly followed by reports from Donovan and co-workers[66,67] who described the direct homopolymerization of styrenic, methacrylic, and acrylamido sulfopropylbetaine derivatives in aqueous media as well as AB diblock and ABA triblock copolymers with *N,N*-dimethylacrylamide. MPC has also been (co)polymerized by RAFT; Yusa et al.[68] described a detailed study of the synthesis and self-association of AB diblock copolymers of MPC with *n*-butyl methacrylate. In addition to MPC, Stenzel et al.[69] reported the RAFT polymerization of 2-(acryloyloxy-)ethyl phosphorylcholine and the ability to form biocompatible nanocontainers.

While MPC has been copolymerized via RAFT with a hydrophobic comonomer, this technique has not been utilized in the preparation of new water-soluble stimulus-responsive block copolymers. To address this, we describe herein the synthesis of a new pH-responsive monomer and the block copolymerization of MPC with a variety of stimulus-responsive, or "smart", neutral, ionic, and sulfobetaine comonomers. The comonomers were chosen to yield a range of materials exhibiting pH, temperature, or salt responsive properties that were anticipated to undergo reversible self-assembly in aqueous media as a function of such applied stimuli.

Experimental Section

All reagents were purchased from the Aldrich Chemical Co. at the highest available purity and used as received unless noted otherwise. *N,N*-Diethylacrylamide was purchased from Polysciences Inc. and purified by distillation. The sulfobetaine monomer, *N*-(3-sulfopropyl)-*N*-methacrylooxyethyl-*N,N*-dimethylammonium betaine (DMAPS), was prepared from the reaction between 2-(dimethylamino)ethyl methacrylate and 1,3-propanesultone in THF at ambient temperature.[25] 4-Cyanopentanoic acid dithiobenzoate,[70] 2-(methacryloyloxy)ethyl phosphorylcholine,[10] and 4-vinylbenzoic acid[70] were prepared according to literature procedures. 4,4′-Azobis(4-cyanovaleric acid) (V-501) was purified by recrystallization from MeOH and stored at −20 °C until needed.

Synthesis of *N,N*-Di-*n*-propyl-4-vinylbenzylamine (DnPBVA). A mixture of 4-vinylbenzyl chloride (29.54 g, 0.194 mol), di-*n*-propylamine amine (50.0 g, 0.387 mol), methanol (50.0 mL, HPLC grade), and a small amount of phenothiazine were added to a 500 mL round-bottom flask equipped with a magnetic stirring bar and a western condenser. The solution was then refluxed for 14 h. Subsequently, methanol was removed using a rotary evaporator. The residue was then dissolved in 4.0 M HCl (100 mL), and this solution was washed three times with diethyl ether (3 × 100 mL). NaOH was then added to the aqueous phase until the solution became slightly basic, after which it was washed three times with diethyl ether (3 × 100 mL). The ether washings were combined and the solvent was removed using a rotary evaporator to give a crude product yield of 76%. The target monomer was purified via fractional distillation (bp of ∼80 °C at ∼1 mbar).

Homopolymerization of 2-(Methacryloyloxy)ethyl Phosphorylcholine (MPC). To a Schlenk flask, equipped with a magnetic stir bar were added MPC (3.0 g, 10.2 mmol), 4-cyanopentanoic acid dithiobenzoate (CTP; 28 mg, 0.10 mmol), V-501 (5.6 mg, 2.0×10^{-2} mmol), deionized H_2O (15.0 g), and 5 wt % $NaHCO_3$ solution (336 mg). The mixture was then stirred for at least 4 h in an ice-bath to ensure complete dissolution of CTP and V-501. The solution was then purged with nitrogen prior to immersion in a preheated oil-bath at 70 °C. After 2 h, the polymerization was stopped via rapid cooling and exposure to air. The polymerization solution was then dialyzed against deionized water for 12 h with 3 changes of the deionized water. Homopolymer was then recovered by freeze-drying, yielding 1.7 g of material (yield of 56.7%).

Synthesis of Poly(MPC-block-4-vinylbenzoic acid), 50:50. All AB diblock copolymers were prepared using the same general approach. Any differences in reaction medium or polymerization temperature are noted in Table 1. Below is detailed the synthesis of a poly(MPC-*block*-4-vinylbenzoic acid) with a target molar composition of 50:50 as a representative example.

A mixture of polyMPC (0.5 g, equivalent to 1.69 mmol of MPC repeat units), 4-vinylbenzoic acid (VBZ; 0.251 g, 1.69 mmol), V-501 (2.8 mg, 9.93×10^{-3} mmol), Na_2CO_3 (180 mg, 1.70 mmol), and deionized H_2O (6.8 g) were added to a Schlenk flask equipped with a magnetic stir bar. The mixture was then stirred for at least 4 h in an ice-bath to ensure complete dissolution of V-501 and VBZ. The solution was then purged with nitrogen prior to immersion in a preheated oil-bath at 80 °C for 12 h. The polymerization was stopped by rapid cooling and exposure to air. The copolymer solution was then was dialyzed against deionized H_2O for 6 h with three changes of the deionized water. The polymer was recovered by freeze-drying.

Sample Preparation for Dynamic Light Scattering Experiments. Samples for dynamic light scattering were prepared as follows: 1.0 wt % solutions were prepared in 5 mL scintillation vials using the appropriate aqueous solution. The solution was then filtered through a Millex syringe filter with a pore size of 0.45 μm and 0.35 mL of the filtered solution was transferred to a polystyrene cuvette using a Rainin P1000 micro Pipette.

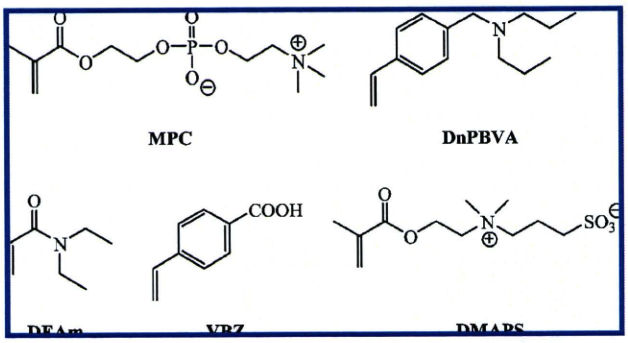

Figure 1. Chemical structures of monomers used in this study.

General Instrumentation. ^{1}H (300 MHz) NMR and ^{13}C (75 MHz) NMR spectra were recorded on a Bruker 300 53 nm spectrometer in appropriate deuterated solvents or solvent mixtures. Aqueous size exclusion chromatography experiments were conducted on a Viscotek system comprised of a Viscotek VE1122 pump, Viscotek VE3580 RI detector, a Viscotek viscoGEL PW_{XL} guard column followed by a series of two viscoGEL columns (G5000PW_{XL} +G4000 PW_{XL}), in 0.25 M NaBr solution, which was degassed prior to use at a flow rate of 1.0 mL/min. The columns were calibrated with a series of narrow molecular weight distribution PEO/PEG standards. Data was manipulated using the Omnisec V4.1 software. Dynamic light scattering (DLS) experiments were conducted on a Malvern Instruments Zetasizer Nano-ZS (red badge) instrument operating with a 633 nm laser. Data was collected and processed with the Dispersion Technology software V5.10.

Results and Discussion

With the aim of preparing and examining a range of new water-soluble, stimulus-responsive block copolymers based on the biocompatible building block 2-(methacryloyloxy)ethyl phosphorylcholine (MPC), a new pH-responsive styrenic monomer was initially prepared, Figure 1. *N,N-n*-Propyl-4-vinylbenzylamine (DnPBVA) was prepared in a straightforward manner from the reaction between 4-vinylbenzylchloride and di-*n*-propylamine and isolated in good yield. The structure of the product was confirmed via a combination of ^{1}H/^{13}C NMR and FTIR spectroscopies. Figure 2 shows the ^{1}H (a) and ^{13}C (b) NMR spectra of DnPBVA, recorded in $CDCl_3$, with peak assignments, verifying structure and purity.

With the exception of *N,N*-diethylacrylamide (DEAm), all other monomers were prepared according to established literature procedures. With all monomers in hand, a polyMPC (PMPC) homopolymer was prepared according to the method of Yusa et al.,[68] Scheme 1.

Homopolymerization of MPC was conducted in water for 2 h at 70 °C using the CTP/V-501 RAFT chain transfer agent (CTA)/initiator combination, with a target M_n of 30000 at quantitative conversion. The resulting MPC homopolymer was purified by dialysis against deionized water for 12 h and subsequently analyzed via a combination of NMR spectroscopy and aqueous size exclusion chromatography (ASEC).

Figure 3a shows the ASEC trace of the purified MPC homopolymer. The chromatogram is unimodal and symmetric, and the homopolymer has an experimentally determined M_n, relative to narrow molecular weight poly(ethylene oxide) standards of 12100, with a corresponding polydispersity index (M_w/M_n) of 1.12. Figure 3b shows the ^{1}H NMR spectrum, recorded in D_2O, of the same MPC homopolymer. Importantly, the resonances associated with the phenyl group of the dithioester end-group are visible and therefore facilitates the determination of the absolute molecular weight. Assuming one phenyl group per polymer chain, a comparison of the integral associated with the phenyl hydrogens with those labeled c yields a calculated absolute M_n of 25400.

Having verified the ability to prepare PMPC in a controlled manner directly in aqueous media, AB diblock copolymers of varying molar composition were prepared with a range of comonomers from different monomer families with different aqueous solution characteristics. For example, homopolymers prepared from DEAm are readily soluble in water at ambient temperature but possess a lower critical solution temperature (LCST) of about 32 °C, essentially identical to the more commonly studied poly(*N*-isopropylacrylamide). Homopolymers derived from VBZ are pH-responsive. Specifically, when ionized, that is, at intermediate-to-high solution pH, homopolymers of VBZ are readily water-soluble. However, in the free acid form, at low pH, such materials undergo a distinct hydrophilic-to-hydrophobic phase transition and become insoluble. We, and others, have previously taken advantage of this pH-trigger in the synthesis of copolymers capable of undergoing pH-induced reversible self-assembly.[50,51,70,71] Homopolymers of DnPBVA likewise exhibit pH-dependent solubility characteristics, although it is opposite to that exhibited by materials containing VBZ, that is, such materials are hydrophilic at low pH when the amine resides are protonated but become hydrophobic when deprotonated. Such behavior is entirely consistent with the structurally similar monomer *N,N*-dimethylvinylbenzylamine.[70] Finally, homopolymers derived from the sulfobetaine monomer DMAPS possess electrolyte responsive features in water.[2,28] Generally, polymeric betaines exhibit limited-to-zero solubility in pure water due to the formation of an ionically cross-linked network-like structure. The addition of a small molecule electrolyte, such as NaCl, at some critical concentration effectively screens these ionic interactions resulting in dissolution. Once in solution, the addition of further salt results in a second, less pronounced conformational effect. In contrast to polyelectrolytes, which undergo chain contraction with added electrolyte, polymeric betaines undergo chain expansion, a phenomena referred to as the *antipolyelectrolyte effect*.[1] With respect to DMAPS, it is the former, more pronounced, effect that is of interest.

Table 1 gives a summary of the AB diblock copolymers that were prepared, their targeted and measured molar compositions, and M_n and polydispersity indices. Several points are worth highlighting. The varied, and sensitive, aqueous solution behavior of the target comonomers/polymers requires careful identification of suitable conditions for effective block copolymerization. The polymerization conditions noted were those found to give acceptable control/kinetics, conversions, and low PDIs. In all instances, V-501 was used as the source of primary radicals at a ratio of 3:1 thiocarbonylthio end-group/initiator. In the case of block copolymers with DEAm, Table 1, entries 1 and 2, copolymerizations were performed at 60 °C in MeOH at a total concentration of 25 wt %. In fact, MeOH is a convenient solvent for MPC and its copolymers and is commonly employed in ATRP syntheses.[30,31,72] DEAm can also be copolymerized in water although this requires a low temperature initiator since, as noted above, PDEAm has an LCST of about 32 °C. Similar polymerization conditions were used for one of the block copolymers with DMAPS, Table 1, entry 6, thus negating the need for added electrolyte in the case of aqueous based polymerization although this is also a feasible approach, Table 1, entry 7. In the case of VBZ block copolymers, Table 1, entries 3 and 4, syntheses were performed in water under

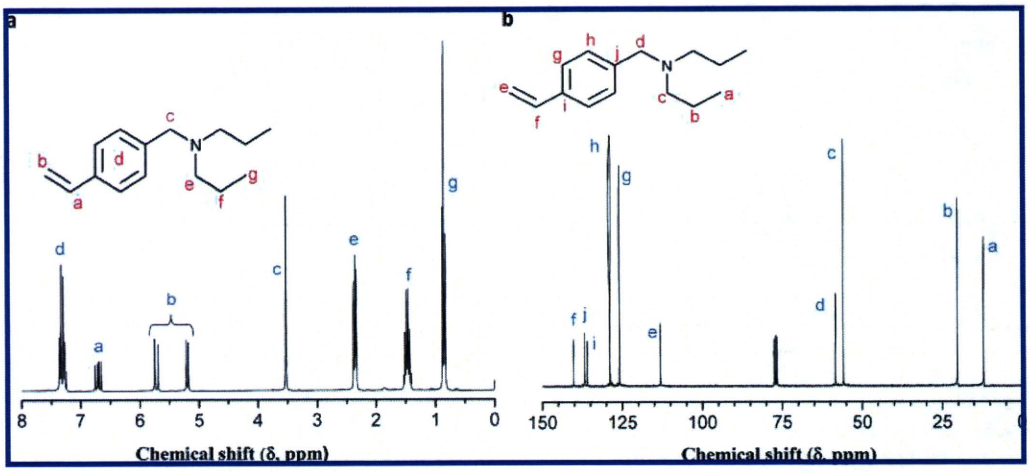

Figure 2. ^{1}H (a) and ^{13}C (b) NMR spectra, recorded in $CDCl_3$, of *N,N*-di-*n*-propylbenzylvinylamine.

Scheme 1. Synthetic Outline for the Preparation of a PMPC Macro-CTA

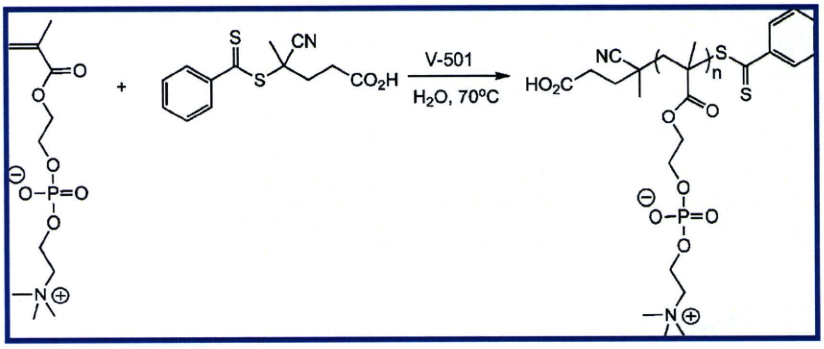

slightly basic conditions although at a lower concentration of 10 wt % and slightly higher reaction temperature of 80 °C. In the case of the block copolymer with DnPBVA, Table 1, entry 5, copolymerization proceeded smoothly in 2,2,2-trifluoroethanol (TFE) at a concentration of 10 wt % and 70 °C. While these synthetic conditions are varied, each of the resulting block copolymers presents a symmetric, unimodal ASEC trace with the final polydispersity indices in the range 1.10−1.24. As representative examples, Figure 4 shows the ASEC traces for the MPC-*b*-DEAm, Table 1, entry 1, and MPC-*b*-DMAPS, Table 1, entry 7, copolymers.

With a series of PMPC-based AB diblock copolymers in hand the aqueous solution properties of specific samples were briefly examined using a combination of ^{1}H NMR spectroscopy and dynamic light scattering (DLS). NMR is particularly useful for monitoring the change in solvation of a particular block under different solution conditions, while DLS is a fast and convenient method for measuring the hydrodynamic properties of copolymers, and aggregates thereof. Figure 5a shows the ^{1}H NMR spectra of the P(MPC-*b*-DEAm) copolymer with a molar composition of 56:44, Table 1, entry 2, at ambient temperature. All the resonances associated with the MPC and DEAm blocks are clearly present. With respect to the DEAm block, the major resonances are those labeled d, e, and f and are associated with the backbone hydrogens, the aza-methylene group, and the methyl hydrogens, respectively. Heating the P(MPC_{56}-*b*-$DEAm_{44}$) copolymer solution in the NMR spectrometer to 50 °C results in an NMR spectrum, Figure 5b, devoid of any signals associated with the DEAm block. Specifically, there are three distinct changes. First, the signals labeled d and e in Figure 5a are completely absent, while there is also a significant decrease in the intensity of the signal at $\delta \sim 1.1$ ppm. These changes are completely consistent with desolvation of the DEAm block. Because there is no evidence of macroscopic precipitation and given the block architecture of the material, such changes are entirely consistent with a self-assembly process yielding, for example, spherical polymeric micelles, Scheme 2. The formation of aggregate structures under these conditions was verified by dynamic light scattering (DLS). Figure 5c shows the measured size distributions for a 1 wt % aqueous solution (0.1 M NaCl) of the P(MPC_{56}-*b*-$DEAm_{44}$) copolymer employed in the NMR study at 22 and 50 °C. At the lower temperature DLS indicates an average hydrodynamic diameter (D_h) of ~6.0 nm, which is entirely consistent with molecularly dissolved polymer chains (unimers) of the measured average molecular weight. In contrast, after heating the solution to 50 °C the size distribution shifts significantly indicating the presence of a species with an average D_h of ~180 nm. Such a dramatic change in the D_h certainly indicates that the AB diblock copolymer is undergoing self-assembly forming an aggregate structure such as a micelle, vesicle, or higher ordered structure. We have not, at this time, attempted to elucidate the exact nature of the aggregate species. However, such assembly is completely reversible. Cooling the solution back down to room temperature results in the disappearance of the large aggregates and the reappearance of the smaller, unimer population. Similarly, temperature cycling in the NMR spectrometer confirms the reversible solvation-desolvation of the DEAm residues (data not shown).

Figures 6−8 show the results from the same series of experiments for the P(MPC_{50}-*b*-VBZ_{50}), P(MPC_{70}-*b*-DnPB-VA_{30}), and the P(MPC_{76}-*b*-$DMAPS_{24}$) copolymers, Table 1, entries 4−6.

Consider first the P(MPC_{50}-*b*-VBZ_{50}) copolymer. Figure 6a shows the ^{1}H NMR spectrum of the block copolymer under

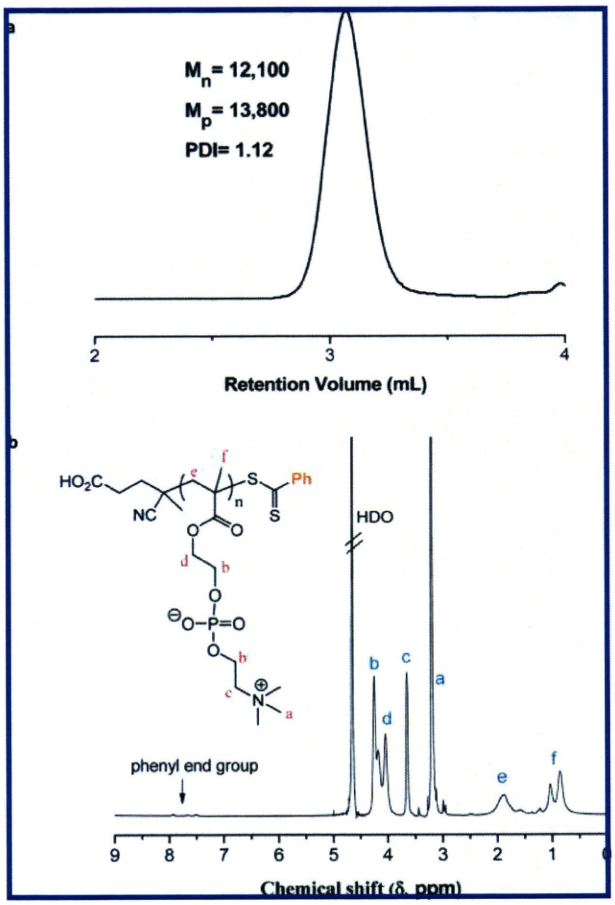

Figure 3. Aqueous size exclusion chromatogram (a; RI signal) of a PMPC homopolymer, and the ^{1}H NMR spectrum (b) of the same homopolymer recorded in D_2O, with peak assignments.

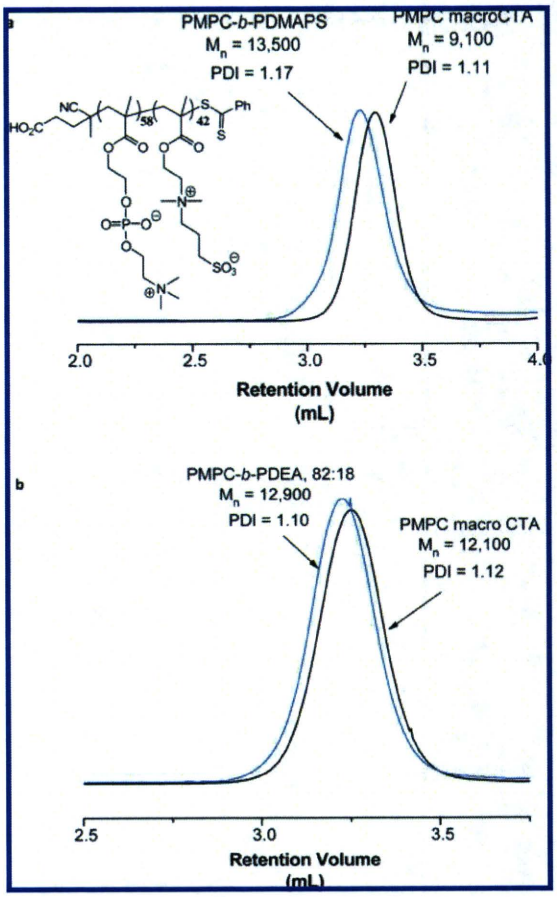

Figure 4. Aqueous size exclusion chromatograms (RI signal) of examples of PMPC-based AB diblock copolymers, P(MPC_{58}-*b*-$DMAPS_{42}$) (a) and P(MPC_{82}-*b*-$DEAm_{18}$) (b), demonstrating successful block copolymer formation.

conditions in which both the MPC and the VBZ blocks are hydrophilic and thus solvated, that is, under basic solution conditions in which the VBZ block is ionized. The key signals associated with MPC are again clearly visible as well as the key resonance for the VBZ block, the two signals spanning $\sim\delta = 6-7.5$ ppm, associated with the four hydrogens of the benzene ring. Acidification of this solution with DCl results in spectrum Figure 6b. The signals associated with MPC are still present but those associated with VBZ are absent. As with the temperature-induced desolvation observed for the P(MPC_{56}-*b*-$DEAm_{44}$) copolymer, this pH-induced change also leads to the formation of nanosized aggregates as evidenced by DLS. Figure 6c shows the measured DLS size distributions for the MPC-*b*-VBZ block copolymer at a concentration of 1 wt %, 22 °C, in 0.2 M NaOH and 0.2 M HCl. Under basic conditions, when both blocks are hydrophilic, DLS indicates the presence of unimers with an average D_h of ~7.0 nm. However, under acidic conditions a rather broad size distribution comparable to that observed for the P(MPC_{56}-*b*-$DEAm_{44}$) copolymer is seen with an average D_h of ~124 nm and a corresponding polydispersity of 0.25. Again, such a size may indicate the presence of vesicles or higher ordered structures as opposed to spherical micelle-like species. Given the similar block copolymer compositions and molecular weights of these P(MPC_{56}-*b*-$DEAm_{44}$) and P(MPC_{50}-*b*-VBZ_{50}) copolymers, it is perhaps not surprising that they behave similarly in their amphiphilic forms even though such behavior is induced by a different external stimulus. The P(MPC_{70}-*b*-$DnPBVA_{30}$) copolymer also exhibits pH-induced self-assembly characteristics although the pH-trigger is reversed.

As noted above, the DnPBVA residues are hydrophilic at low pH but hydrophobic at intermediate-to-high pH. Figure 7a shows the ^{1}H NMR spectrum of the P(MPC_{70}-*b*-$DnPBVA_{30}$) under acidic conditions where both blocks are hydrophilic and solvated. The main, identifiable, signals associated with the DnPBVA block are those associated with the aromatic ring at $\sim\delta = 6-7.2$ ppm as well as the signal at $\sim\delta = 2.7$ ppm. Under basic conditions, both of these key signals disappear consistent with the pH-induced hydrophilic−hydrophobic transition of the DnPBVA residues. DLS again confirms the occurrence of a self-assembly process with this change in solution pH. For a 1 wt % solution of the P(MPC_{70}-*b*-$DnPBVA_{30}$) at 22 °C, a unimers distribution with an average D_h of ~6 nm is observed. Deprotonation of the DnPBVA residues renders them hydrophobic and self-assembly occurs yielding aggregates with a D_h of ~22 nm. This size is much smaller than those observed for either the P(MPC_{56}-*b*-$DEAm_{44}$) or P(MPC_{50}-*b*-VBZ_{50}) copolymers, although it must be noted that the copolymer composition is significantly different. Finally, the P(MPC_{76}-*b*-$DMAPS_{24}$) copolymer was examined with respect to the effect of electrolyte on solubility/self-assembly. In the case of the NMR experiments, little or no change was observed in peak intensities when spectra were recorded in the presence and absence of electrolyte indicating that the DMAPS block was still in a solvated, although perhaps somewhat reduced, state. In contrast, DLS experiments did indicate the presence of aggregate structures for the block copolymer in deionized water. Figure 8 shows

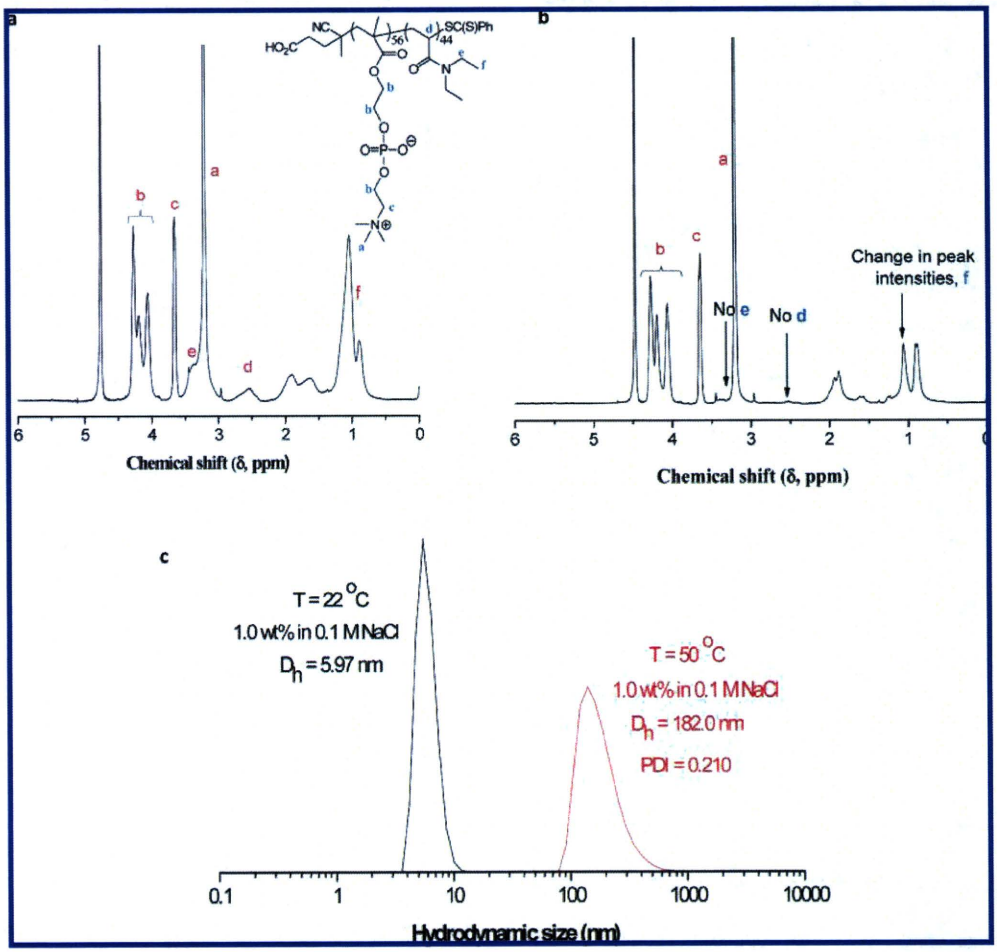

Figure 5. ^{1}H NMR spectra, recorded in D_2O, of the P(MPC_{56}-*b*-$DEAm_{44}$) at ambient temperature (a) and at 50 °C (b) demonstrating the desolvation of the DEAm block as a function of change in solution temperature and the intensity-average size distributions measured by dynamic light scattering (c) as a function of temperature highlighting the formation of aggregates.

Scheme 2. Idealized, Reversible Self-Assembly, with the Possible Formation of Either Micelles or Vesicles, of "Smart" AB Diblock Copolymers Based on PMPC

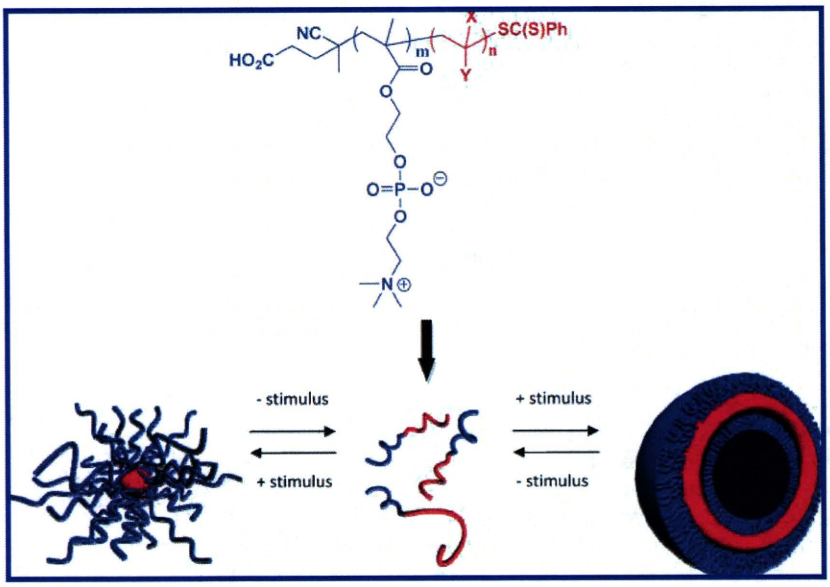

the measured size distributions for the P(MPC_{76}-*b*-$DMAPS_{24}$) copolymer in 0.5 M NaCl and deionized water at a concentration of 1 wt % at 22 °C. In the electrolyte solution unimers are observed with an average D_h of ~6 nm. In contrast, when dissolved directly in deionized water aggregates are observed with an average D_h of 174 nm. A more detailed, fundamental study of the effect of block copolymer composition on the self-assembly properties of these copolymers is currently underway.

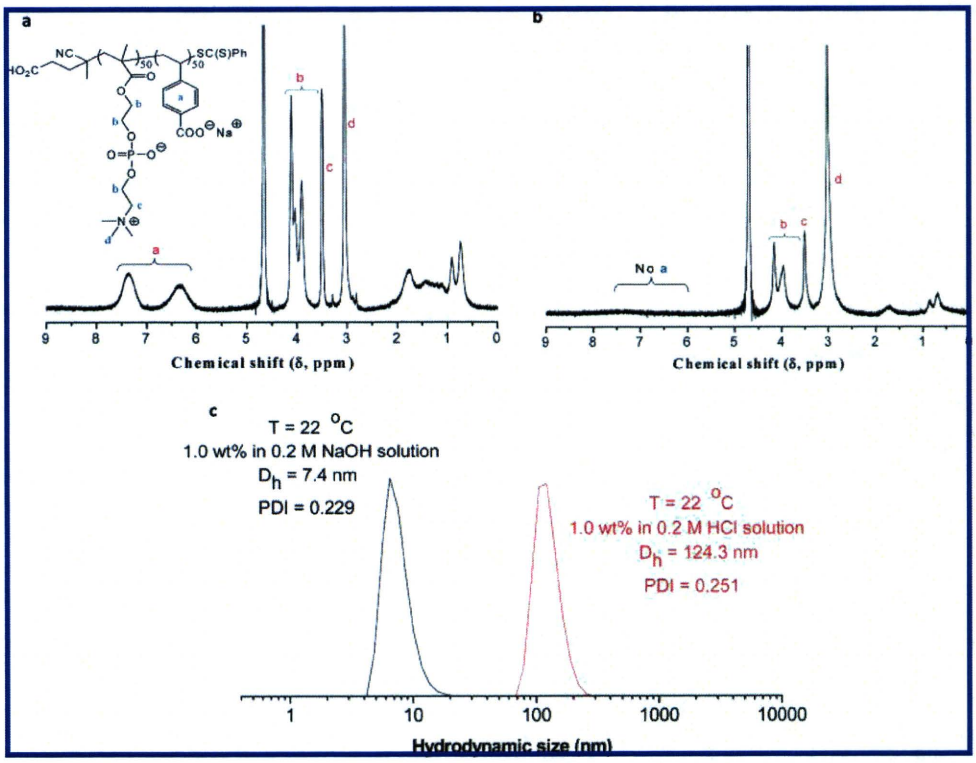

Figure 6. ^{1}H NMR spectra, recorded in D_2O, of the P(MPC_{50}-*b*-VBZ_{50}) at ambient temperature under basic conditions (a) and under acidic conditions (b), demonstrating the desolvation of the VBZ block as a function of change in solution pH and the intensity-average size distributions measured by dynamic light scattering (c) as a function of pH highlighting the formation of aggregates.

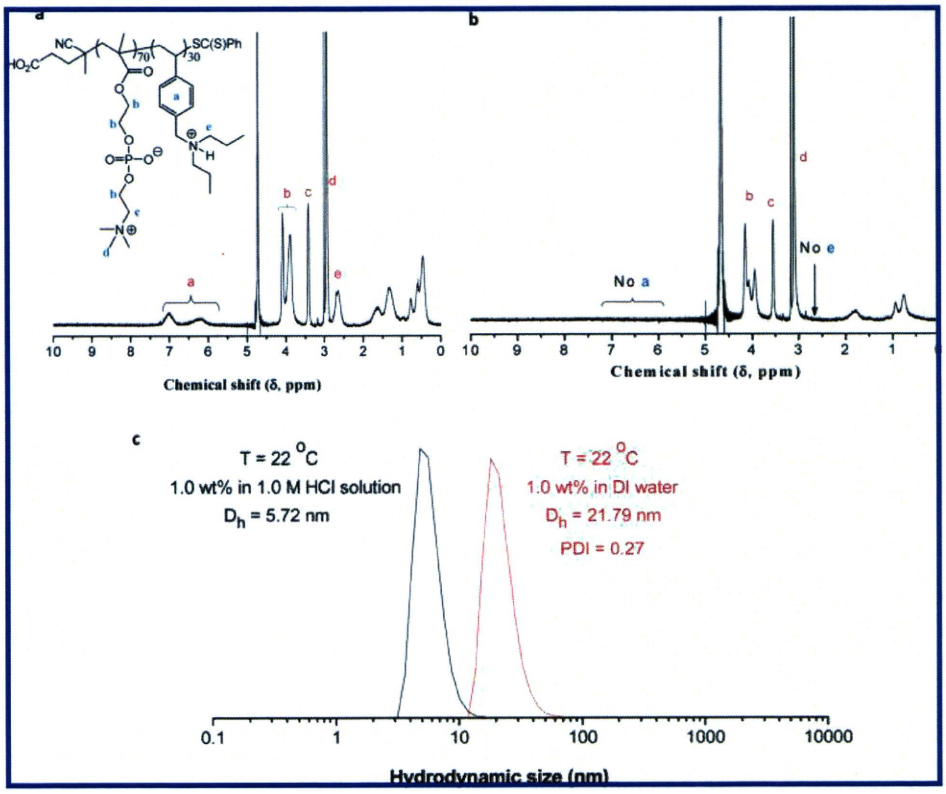

Figure 7. ^{1}H NMR spectra, recorded in D_2O, of the P(MPC_{70}-*b*-$DnPBVA_{30}$) at ambient temperature under acidic conditions (a) and under neutral/basic conditions (b), demonstrating the desolvation of the DnPBVA block as a function of change in solution pH and the intensity-average size distributions measured by dynamic light scattering (c) as a function of pH highlighting the formation of aggregates.

Summary and Conclusions

We have demonstrated herein that reversible addition-fragmentation chain transfer (RAFT) radical polymerization is a convenient method for the synthesis of a range of AB diblock copolymers based on the PMPC with a range of "smart" comonomers. Employing a MPC macro-CTA, well-

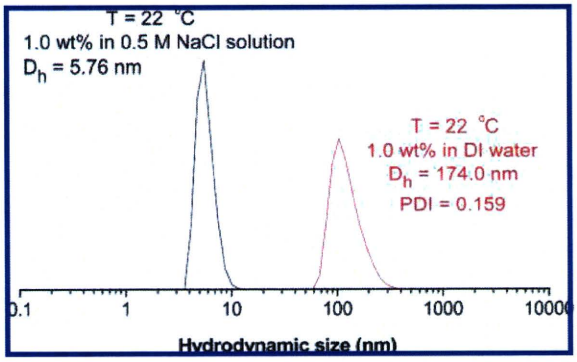

Figure 8. Experimentally determined hydrodynamic size distributions of a 1 wt % solution of the P(MPC_{76}-*b*-$DMAPS_{24}$) copolymer in 0.5 M NaCl and deionized water, demonstrating the ability to form self-assembled aggregates.

defined AB diblock copolymers of varying molar composition and narrow molecular weight distribution with *N*,*N*-diethylacrylamide, 4-vinylbenzoic acid, *N*,*N*-di-*n*-propylbenzylvinylamine, and *N*-(3-sulfopropyl)-*N*-methacrylooxyethyl-*N*,*N*-dimethylammonium betaine were prepared in protic media. These comonomers were chosen to yield block copolymers that were capable of undergoing stimulus induced self-assembly in aqueous media. Indeed, we demonstrated that such PMPC-based block copolymers are able to undergo self-assembly processes as a functional of either a change in solution temperature, pH, or electrolyte concentration. Preliminary evaluation of the self-assembly properties using a combination of ^{1}H NMR spectroscopy and dynamic light scattering showed that when molecularly dissolved the block copolymers had average hydrodynamic diameters in of ~6−7 nm. In contrast, and under the appropriate applied external stimulus, aggregates in the range ~22−180 nm. Such self-assembly is completely reversible and removal of the applied stimulus results in a return to the unimeric state.

Acknowledgment. A.B.L. would like to thank the Materials Research Science and Engineering Center at USM (DMR-0213883) for funding this work in the form of a stipend for B.Y.

References and Notes

(1) Lowe, A. B.; McCormick, C. L. *Chem. Rev.* **2002**, *102*, 4177–4190.
(2) Kudaibergenov, S.; Jaeger, W.; Laschewsky, A. *Adv. Polym. Sci.* **2006**, *201*, 157–224.
(3) Salamone, J. C.; Volksen, W.; Israel, S. C.; Olson, A. P.; Raia, D. C. *Polymer* **1977**, *18*, 1058–1062.
(4) Monroy Soto, V. M.; Galin, J. C. *Polymer* **1984**, *25*, 121–128.
(5) Favresse, P.; Laschewsky, A. *Polymer* **2001**, *42*, 2755–2766.
(6) Kathmann, E. E.; White, L. A.; McCormick, C. L. *Polymer* **1997**, *38*, 879–886.
(7) Bonte, N.; Laschewsky, A. *Polymer* **1996**, *37*, 2011–2019.
(8) Kathmann, E. E.; White, L. A.; McCormick, C. L. *Polymer* **1997**, *38*, 871–878.
(9) Nagaya, J.; Uzawa, H.; Minoura, N. *Macromol. Rapid Commun.* **1999**, *20*, 573–576.
(10) Ishihara, K.; Ueda, T.; Nakabayashi, N. *Polym. J.* **1990**, *22*, 355–360.
(11) Ishihara, K.; Ziats, N. P.; Tierney, B. P.; Nakabayashi, N.; Anderson, J. M. *J. Biomed. Mater. Res.* **1991**, *25*, 1397–1407.
(12) Hasegawa, T.; Iwasaki, Y.; Ishihara, K. *J. Biomed. Mater. Res.* **2002**, *63*, 333–341.
(13) Lobb, E. J.; Ma, I.; Billingham, N. C.; Armes, S. P.; Lewis, A. L. *J. Am. Chem. Soc.* **2001**, *123*, 7913–7914.
(14) Ishihara, K.; Iwasaki, Y.; Fiujiike, A.; Kurita, K.; Nakabayashi, N. *J. Polym. Sci., Part A: Polym. Chem.* **1996**, *34*, 199–205.
(15) Oishi, T.; Fukuda, T.; Uchiyama, H.; Kondou, F.; Hoe, H.; Tsutsumi, H. *Polymer* **1997**, *38*, 3109–3115.
(16) Sugiyama, K.; Ohga, K.; Aoki, H. *Macromol. Chem. Phys.* **1995**, *196*, 1907–1916.
(17) Kros, A.; Gerritsen, M.; Murk, J.; Jansen, J. A.; Sommerdijk, N. A. J. M. *J. Polym. Sci., Part A: Polym. Chem.* **2001**, *39*, 468–474.
(18) Pujol-Fortin, M.-L.; Galin, J. C. *Macromolecules* **1991**, *24*, 4523–4530.
(19) Pujol-Fortin, M.-L.; Galin, J. C. *Polymer* **1994**, *35*, 1462–1472.
(20) Chrisment, J.; Galin, M.; Galin, J. C. *New J. Chem.* **1995**, *19*, 303–311.
(21) Galin, J. C.; Galin, M. *J. Polym. Sci., Part A: Polym. Phys.* **1995**, *33*, 2033–2043.
(22) Grassl, B.; Francois, J.; Billon, L. *Polym. Int.* **2001**, *50*, 1162–1169.
(23) Ladenheim, H.; Morawetz, H. *J. Polym. Sci.* **1957**, *26*, 251–254.
(24) Hart, R.; Timmerman, D. *J. Polym. Sci.* **1958**, *28*, 638–640.
(25) Lowe, A. B.; Billingham, N. C.; Armes, S. P. *Chem. Commun.* **1996**, 1555–1556.
(26) Tuzar, Z.; Popisil, H.; Plestil, J.; Lowe, A. B.; Baines, F. L.; Billingham, N. C.; Armes, S. P. *Macromolecules* **1997**, *30*, 2509–2512.
(27) Bütün, V.; Bennett, C. E.; Vamvakaki, M.; Lowe, A. B.; Billingham, N. C.; Armes, S. P. *J. Mater. Chem.* **1997**, *7*, 1693–1695.
(28) Lowe, A. B.; Billingham, N. C.; Armes, S. P. *Macromolecules* **1999**, *32*, 2141–2148.
(29) Lowe, A. B.; Vamvakaki, M.; Wassall, M. A.; Wong, L.; Billingham, N. C.; Armes, S. P.; Lloyd, A. W. *J. Biomed. Mater. Res.* **2000**, *52*, 88–94.
(30) Ma, I.; Lobb, E. J.; Billingham, N. C.; Armes, S. P.; Lewis, A. L.; Lloyd, A. W. *Macromolecules* **2002**, *35*, 9306–9314.
(31) Ma, Y.; Tang, Y.; Billingham, N. C.; Armes, S. P.; Lewis, A. L.; Lloyd, A. W.; Salvage, J. P. *Macromolecules* **2003**, *36*, 3475–3484.
(32) Licciardi, M.; Tang, Y.; Billingham, N. C.; Armes, S. P.; Lewis, A. L. *Biomacromolecules* **2005**, *6*, 1085–1098.
(33) Kimura, M.; Takai, M.; Ishihara, K. *J. Biomed. Mater. Res.* **2007**, *80A*, 45–54.
(34) Sawada, S.-i.; Sakaki, S.; Iwasaki, Y.; Nakabayashi, N.; Ishihara, K. *J. Biomed. Mater. Res* **2003**, *64A*, 411–416.
(35) Ueda, T.; Oshida, H.; Kurita, K.; Ishihara, K.; Nakabayashi, N. *Polym. J.* **1992**, *24*, 1259–1269.
(36) Ishihara, K.; Aragaki, R.; Ueda, T.; Watenabe, A.; Nakabayashi, N. *J. Biomed. Mater. Res.* **1990**, *24*, 1069–1077.
(37) Lewis, A. L.; Hughes, P. D.; Kirkwood, L. C.; Leppard, S. W.; Redman, R. P.; Tolhurst, L. A.; Stratford, P. W. *Biomaterials* **2000**, *21*, 1847–1859.
(38) West, S. L.; Salvage, J. P.; Lobb, E. J.; Armes, S. P.; Billingham, N. C.; Lewis, A. L.; Hanlon, G. W.; Lloyd, A. W. *Biomaterials* **2004**, *25*, 1195–1204.
(39) Moro, T.; Takatori, Y.; Ishihara, K.; Konno, T.; Takigawa, Y.; Matsushita, T. *Nat. Mater.* **2004**, *3*, 829–836.
(40) Fujii, K.; Matsumoto, H.; Koyama, Y.; Iwasaki, Y.; Ishihara, K.; Takakuda, K. *J. Vet. Med. Sci.* **2008**, *70*, 167–173.
(41) Rankin, D. A.; Lowe, A. B. *Macromolecules* **2008**, *41*, 614–622.
(42) Colak, S.; Tew, G. N. *Macromolecules* **2008**, *41*, 8436–8440.
(43) Moad, G.; Rizzardo, E.; Thang, S. H. *Aust. J. Chem.* **2005**, *58*, 379–410.
(44) McCormick, C. L.; Lowe, A. B. *Acc. Chem. Res.* **2004**, *37*, 312–325.
(45) Lowe, A. B.; McCormick, C. L. *Prog. Polym. Sci.* **2007**, *32*, 283–351.
(46) Barner-Kowollik, C.; Buback, M.; Charleux, B.; Coote, M. L.; Drache, M.; Fukuda, T.; Goto, A.; Klumperman, B.; Lowe, A. B.; McCleary, J. B.; Moad, G.; Monteiro, M. J.; Sanderson, R. D.; Tonge, M. P.; Vana, P. *J. Polym. Sci., Part A: Polym. Chem.* **2006**, *44*, 5809–5831.
(47) Favier, A.; Charreyre, M.-T. *Macromol. Rapid Commun.* **2006**, *27*, 653–692.
(48) Mitsukami, Y.; Hashidzume, A.; Yusa, S.-i.; Morishima, Y.; Lowe, A. B.; McCormick, C. L. *Polymer* **2006**, *47*, 4330–4340.
(49) Lowe, A. B.; Wang, R.; Tiriveedhi, V.; Butko, P.; McCormick, C. L. *Macromol. Chem. Phys.* **2007**, *208*, 2339–2347.
(50) Wang, R.; Lowe, A. B. *J. Polym. Sci., Part A: Polym. Chem.* **2007**, *45*, 2468–2483.
(51) Lowe, A. B.; Torres, M.; Wang, R. *J. Polym. Sci., Part A: Polym. Chem.* **2007**, *45*, 5864–5871.
(52) Sumerlin, B. S.; Lowe, A. B.; Thomas, D. B.; Convertine, A. J.; Donovan, M. S.; McCormick, C. L. *J. Polym. Sci., Part A: Polym. Chem.* **2004**, *42*, 1724–1734.
(53) Gondi, S. R.; Vogt, A. P.; Sumerlin, B. S. *Macromolecules* **2007**, *40*, 474–481.
(54) Lowe, A. B.; Wang, R. *Polymer* **2007**, *48*, 2221–2230.
(55) Wang, R.; McCormick, C. L.; Lowe, A. B. *Macromolecules* **2005**, *38*, 9518–9525.

(56) Convertine, A. J; Lokitz, B. S.; Vasilieva, Y.; Myrick, L. J.; W., S. C.; Lowe, A. B.; McCormick, C. L. *Macromolecules* **2006**, *39*, 1724–1730.
(57) Chan, J. W.; Yu, B.; Hoyle, C. E.; Lowe, A. B. *Chem. Commun.* **2008**, 4959–4961.
(58) Convertine, A. J.; Lokitz, B. S.; Lowe, A. B.; Scales, C. W.; Myrick, L. J.; McCormick, C. L. *Macromol. Rapid Commun.* **2005**, *26*, 791–795.
(59) Li, M.; De, P.; Gondi, S. R.; Sumerlin, B. S. *J. Polym. Sci., Part A: Polym. Chem.* **2008**, *46*, 5093–5100.
(60) Scales, C. W.; Vasilieva, Y.; Convertine, A. J.; Lowe, A. B.; McCormick, C. L. *Biomacromolecules* **2005**, *6*, 1846–1850.
(61) Vasilieva, Y.; Scales, C. W.; Thomas, D. B.; Ezell, R. G.; Lowe, A. B.; Ayres, N.; McCormick, C. L. *J. Polym. Sci., Part A: Polym. Chem.* **2005**, *43*, 3141–3152.
(62) Pound, G.; Aguesse, F.; McCleary, J. B.; Lange, R. F. M.; Klumperman, B. *Macromolecules* **2007**, *40*, 8861–8871.
(63) Mori, H.; Ookuma, H.; Endo, T. *Macromolecules* **2008**, *41*, 6925–6934.
(64) Yasser, A.; Andreas, G.; Seema, A. *Macromol. Rapid Commun.* **2007**, *28*, 1923–1928.
(65) Arotcarena, M.; Heise, B.; Ishaya, S.; Laschewsky, A. *J. Am. Chem. Soc.* **2002**, *124*, 3787–3793.
(66) Donovan, M. S.; Sumerlin, B. S.; Lowe, A. B.; McCormick, C. L. *Macromolecules* **2002**, *35*, 8663–8666.
(67) Donovan, M. S.; Lowe, A. B.; Sanford, T. A.; McCormick, C. L. *J. Polym. Sci., Part A: Polym. Chem.* **2003**, *41*, 1262–1281.
(68) Yusa, S.-i.; Fukuda, K.; Yamamoto, T.; Ishihara, K.; Morishima, Y. *Biomacromolecules* **2005**, *6*, 663–670.
(69) Stenzel, M. H.; Barner-kowollik, C.; Davis, T. P.; Dalton, H. M. *Macromol. Biosci.* **2005**, *4*, 445–453.
(70) Mitsukami, Y.; Donovan, M. S.; Lowe, A. B.; McCormick, C. L. *Macromolecules* **2001**, *34*, 2248–2256.
(71) Gabaston, L. I.; Furlong, S. A.; Jackson, R. A.; Armes, S. P. *Polymer* **1999**, *40*, 4505–4514.
(72) Madsen, J.; Armes, S. P.; Lewis, A. L. *Macromolecules* **2006**, *39*, 7455–7457.

BM8014945

Biomaterials 30 (2009) 4930–4938

Contents lists available at ScienceDirect

Biomaterials

journal homepage: www.elsevier.com/locate/biomaterials

Protein adsorption and cell adhesion on cationic, neutral, and anionic 2-methacryloyloxyethyl phosphorylcholine copolymer surfaces

Yan Xu*, Madoka Takai*, Kazuhiko Ishihara

Department of Materials Engineering, School of Engineering and Center for NanoBio Integration, The University of Tokyo, 7-3-1, Hongo, Bunkyo-ku, Tokyo 113-8656, Japan

ARTICLE INFO

Article history:
Received 3 May 2009
Accepted 4 June 2009
Available online 26 June 2009

Keywords:
2-Methacryloyloxyethyl phosphorylcholine polymer
Coating
Surface charge
Protein adsorption
Cell adhesion

ABSTRACT

Protein adsorption and cell adhesion on cationic, neutral, and anionic water-soluble 2-methacryloyloxyethyl phosphorylcholine (MPC) copolymer surfaces were compared. These model MPC copolymers coated SiO_2 surfaces exhibited comparable surface ζ-potentials of 26.1 mV, near 0 mV, and −24.2 mV, respectively. X-ray photoelectron spectroscopy analyses indicated the similarities and the differences in the surface composition between the sample surfaces. Atomic force microscopy analyses revealed that the type of the charged moiety did not affect the surface roughness. Static contact angle measurements and dynamic contact angle analyses not only indicated that the surfaces were very hydrophilic in general, but also provided information on the surface mobility and the dominant role of MPC at the surface in aqueous conditions. Comparing with the SiO_2 substrates on which protein seriously adsorbed and cell heavily adhered, three MPC copolymers coated surfaces, despite their different charge properties, exhibited significantly low adsorbed amounts of different proteins having various electrical natures and totally no cell adhesion. This suggested that the incorporation of charged moieties in the MPC copolymers did not significantly inspire both the protein adsorption and cell adhesion. The MPC moieties were predominant at the surface when in contact with aqueous conditions and thereby dominated the bioadsorptions, while the possible effect from electrostatic interactions would be too small and too limited to influence the overall situation. Therefore, these MPC copolymer surfaces can satisfy those biological applications requiring not only electrical but also non-biofouling properties.

1. Introduction

2-Methacryloyloxyethyl phosphorylcholine (MPC) polymers have been widely used to construct non-biofouling surfaces in various biomedical applications as they have been shown to resist both protein adsorption and cell adhesion [1–3]. The MPC unit contains a zwitterionic phospholipid group (i.e. phosphorylcholine (PC)) that is also present in cell membranes and possesses non-thrombogenic property and high biocompatibility. Nevertheless, the widely researched MPC polymers are mainly electrically neutral in nature and the behaviors of protein adsorption and cell adhesion on the electrically charged MPC polymer surfaces have not been fully elucidated.

Lewis et al. have evaluated a cationic MPC copolymer and revealed its potential in the application of drug delivery systems [4]. Others have reported their achievements in the successful development of cationically charged MPC polymers as gene vectors [5–7]. On the one hand, as decided by their purposes, these researches focused on the polymer-DNA complexes formation and the subsequent transfection, and very few touched upon the story of interactions of proteins/cells to the charged MPC polymers. However, this is an essential issue that should be addressed before they are administrated in the body: generally, charged polymers tend to nonspecifically bind proteins and cells due to the electrostatic interactions, which would cause wrong targeting and low efficiency, possibly induce their accumulation in the bloodstream and organs, and may initiate inflammatory responses of the body [8,9]; consequently, these problems seriously restrict and impede the applications of charged polymers in biomedicine. On the other hand, the components of these reported cationic MPC copolymers varied with the research topics. To elucidate the fundamental aspects such as interactions between the proteins/cells and the polymer, comparable model polymers with different electrical natures are very beneficial and necessary.

With the incorporation of an anionic monomer 3-methacryloyloxypropyl sulfonate (PMPS), we previously developed an anionic MPC copolymer, poly(MPC-*co*-*n*-butyl methacrylate (BMA)-*co*-PMPS-*co*-3-methacryloxypropyl trimethoxysilane (MPTMSi)) (referred to as PMBSSi, Fig. 1) [10]. It was revealed that the PMBSSi

* Corresponding authors. Tel.: +81 3 5841 7125; fax: +81 3 5841 8647.
E-mail addresses: xuyan@icl.t.u-tokyo.ac.jp (Y. Xu), takai@mpc.t.u-tokyo.ac.jp (M. Takai).

0142-9612/$ – see front matter © 2009 Elsevier Ltd. All rights reserved.
doi:10.1016/j.biomaterials.2009.06.005

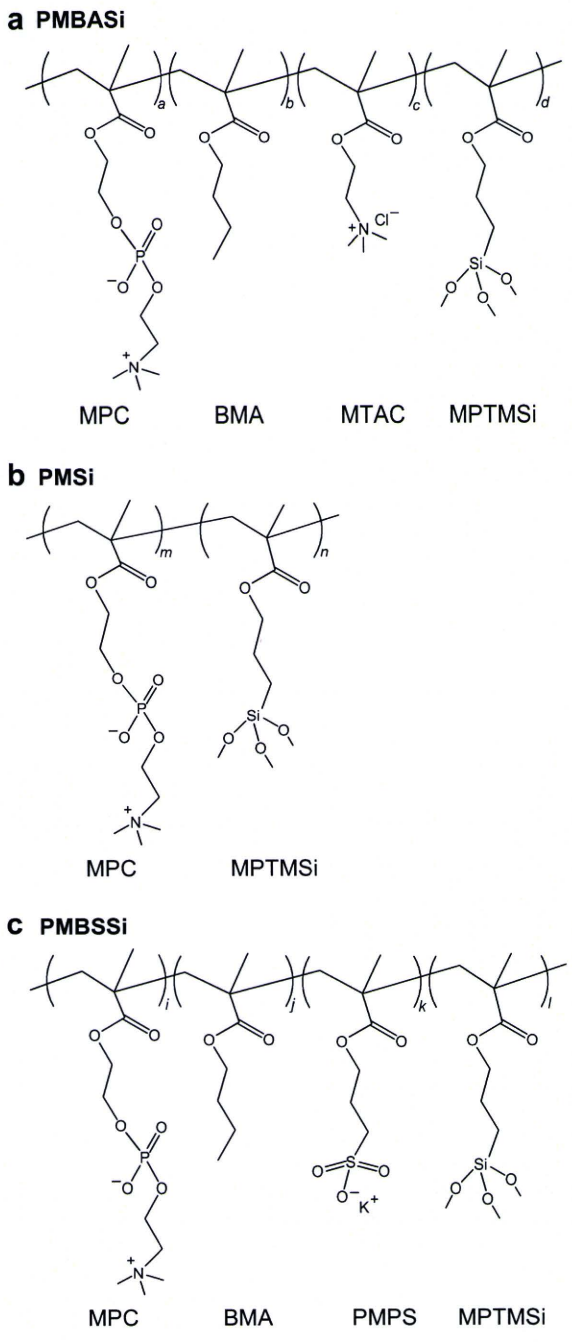

Fig. 1. Chemical structures of (a) PMBASi (cationic), (b) PMSi (neutral), and (c) PMBSSi (anionic).

has high capability to suppress the protein adsorption [11]. The understanding caused us to explore whether the incorporation of cationic charge in an MPC polymer system has the same properties and merits as the incorporation of anionic charge. 2-Methacryloyloxyethyl trimethyl ammonium chloride (MTAC), which contains a cationically charged group, was therefore introduced for this purpose. MTAC was chosen because it not only has reactivity to the other methacrylate monomers such as MPC but also is commercially available and well documented in literature [12,13]. By replacing the anionic PMPS in the PMBSSi with the cationic MATC, recently we have developed a cationic MPC copolymer, which is poly(MPC-*co*-BMA-*co*-MTAC-*co*-MPTMSi) and is referred to as PMBASi (Fig. 1). PMBASi and PMBSSi are comparable on the structure. Like the anionic PMBSSi, the cationic PMBASi is also composed of zwitterionic phospholipid moieties (i.e., MPC), hydrophobic moieties (i.e., BMA), charged moieties (i.e., MTAC), and covalently functional moieties (i.e., MPTMSi), which represent the basic, necessary aspects of a copolymer system and can be used as a model cationic MPC copolymer for research. For comparison, a typical neutral MPC copolymer without incorporation of charge and hydrophobic moieties, that is poly(MPC-*co*-MPTMSi) (referred to as PMSi, Fig. 1), was also synthesized.

Interfacial properties including surface chemistry [14,15], functional groups [16], charge [17–19], roughness [20,21], and wettability [22,23], are generally believed to be closely related to both the protein adsorption and the cell adhesion to a surface. In this study, the behaviors of protein adsorption and cell adhesion on the cationic, neutral, and anionic MPC copolymer surfaces were comparatively investigated from these interfacial aspects. We believe that the information obtained in this study is crucial and meaningful, to clarify the effect of the charge incorporation on an MPC polymer surface, to elucidate the fundamental mechanism of the protein adsorption and cell adhesion to a charged surface, and to explore the potential of the MPC polymers to be applied in the biomedical areas needing charged but non-biofouling surfaces.

2. Materials and methods

2.1. Chemicals, reagents, and proteins

2-Methacryloyloxyethyl phosphorylcholine (MPC) was synthesized as already reported by us elsewhere [1]. *n*-Butyl methacrylate (BMA) (Kanto chemicals, Tokyo, Japan) was distilled before use. 2-Methacryloyloxyethyl trimethylammonium chloride (MTAC) (Wako Pure Chemical, Tokyo, Japan), potassium 3-methacryloyloxypropyl sulfonate (PMPS) (Tokyo Kasei Kogyo Co., Tokyo, Japan), 3-methacryloxypropyl trimethoxysilane (MPTMSi) (Kanto Chemicals), and α,α′-azobisisobutyronitrile (AIBN) (Kanto Chemicals) were commercially purchased as a fine grade. Deuterium oxide (D_2O, 99.8% for NMR spectroscopy) and Ethanol-D (CD_3CD_2OD, 99% for NMR spectroscopy) were purchased from Merck KGaA (Darmstadt, Germany). SiO_2 substrates (thickness 0.5 mm) were obtained from Sendai Quartz and Glass (Sendai, Japan). Pepsin (35.0 kDa, p*I* = 1.0) from porcine stomach mucosa, albumin from bovine serum (BSA, 66.0 kDa, p*I* = 4.7), ribonuclease A (RNase A, 13.7 kDa, p*I* = 9.5) from bovine pancreas, and lysozyme (LYZ, 14.3 kDa, p*I* = 11.0) from chicken egg white were purchased from Aldrich–Sigma (St. Louis, MO, USA). Dulbecco's modified eagle's medium (DMEM), fetal bovine serum (FBS), Dulbecco's phosphate buffered saline (PBS, pH 7.1), and other cell culture reagents were purchased from Invitrogen (Carlsbad, CA, USA).

2.2. Synthesis and characterization of MPC copolymers

Poly (MPC-*co*-BMA-*co*-MTAC-*co*-MPTMSi) (PMBASi, Fig. 1) was synthesized by a conventional radical polymerization technique. Briefly, the desired amounts of MPC, BMA, MTAC, MPTMSi, and AIBN (as initiator) were first dissolved in ethanol in a polymerization flask, and then the copolymerization was performed at 60 °C for 6 h in the flask after sealed. The polymerization product was collected after a reprecipitation from an ether/chloroform (7/3, v/v) mixture solvent. The remaining solvent was removed via a vacuum drying to get a white powder. The structure was identified by ^{1}H NMR spectra (JEOL, 270 MHz, Tokyo, Japan) (CD_3CD_2OD, δ): δ_H = 0.77–0.81 ($-CH_2Si-$), 0.90–1.09 (α-CH_3), 1.19–1.55 ($-CH_3$), 1.84–2.26 ($-CH_2-$), 3.00–3.17 ($-N(CH_3)_3$), 3.24–3.38 ($-OCH_2CH_2OP$), 3.69–4.44 ($-OCH_2-$).

Poly (MPC-*co*-MPTMSi) (PMSi, Fig. 1) was synthesized using the same method with the monomers of MPC and MPTMSi. ^{1}H NMR spectra (D_2O, δ): δ_H = 0.60–0.65 ($-CH_2Si-$), 0.93–1.10 (α-CH_3), 1.14–1.46 ($-CH_2-$), 2.87–3.01 ($-N(CH_3)_3$), 3.54–3.70 ($-OCH_2CH_2OP$), 3.94–4.31 ($-OCH_2-$).

Poly (MPC-*co*-BMA-*co*-PMPS-*co*-MPTMSi) (PMBSSi, Fig. 1) was synthesized using the same method with the monomers of MPC, BMA, PMPS, and MPTMSi. ^{1}H NMR spectra (CD_3CD_2OD, δ): δ_H = 0.60–0.65 ($-CH_2Si-$), 0.90–1.04 (α-CH_3), 1.22–1.37 ($-CH_3$), 1.56–1.83 ($-CH_2-$), 3.15–3.24 ($-N(CH_3)_3$), 3.46–3.68 ($-OCH_2CH_2OP$), 3.97–4.24 ($-OCH_2-$).

The average molecular weight was estimated by a gel permeation chromatography (GPC) system (JASCO, Tokyo, Japan). The solubility was evaluated by dissolving 0.1 g polymer powder in a 10 mL solvent (water and ethanol). The molecular properties of three polymers are summarized in Table 1.

Table 1
Molecular properties of PMBASi, PMSi, and PMBSSi.

Abb.	Composition (mole fraction)[a]	Molecular weight (M_w)[c]	Polydispersity ratio(M_w/M_n)[d]	Solubility[e]	
	[MPC/BMA/X[b]/MPTMSi]			H_2O	EtOH
PMBASi	48/23/18/11	9.9×10^3	1.1	+	+
PMSi	80/0/0/20	9.7×10^3	1.1	+	+
PMBSSi	46/32/9/13	11.8×10^3	1.2	+	+

[a] Determined by ^{1}H NMR.
[b] X is MTAC in PMBASi or PMPS in PMBSSi.
[c] Weight average molecular weight (M_w);determined by GPC, PEO standard.
[d] M_n: number average molecular weight.
[e] Evaluated by dissolving 0.1 g polymer powder in a 10 mL solvent; +: soluble.

2.3. Preparation of covalent coating on SiO_2 substrates

The SiO_2 substrates were first cleaned by ultrasonic rinsing in ethanol and O_2 plasma treatment successively. Then, the cleaned substrates were immersed in 3.00 mg mL^{-1} polymer ethanol solutions for 2 h. After dried under nitrogen, the coated substrates were immediately further dried in vacuo overnight. Before use, the coated substrates were thoroughly rinsed with the distilled water to remove the remaining unreacted molecules, then dried under nitrogen, and dried again in vacuo overnight.

2.4. X-ray photoelectron spectroscopy (XPS) analysis

XPS (Axis-His, Shimadzu/KRATOS, Kyoto, Japan) analyses were made under a high vacuum condition of 1×10^{-9} Torr with MgKα (1253.6 eV) X-ray source. The applied voltage was 12 kV, the electric current was 10 mA, and the employed takeoff angle was 90°. The binding energy (BE) scale was corrected using C_{1s} as a reference at BE = 285 eV. The six elements present in the polymers were identified from their XPS peaks: silicon (Si_{2p}, BE ~ 102 eV), phosphorus (P_{2p}, BE ~ 133 eV), sulfur (S_{2p}, BE ~ 168 eV), carbon (C_{1s}, BE ~ 285 eV), nitrogen (N_{1s}, BE ~ 402 eV), and oxygen (O_{1s}, BE ~ 533 eV).

2.5. Measurement of surface ζ-potential

The measurements of the surface ζ-potentials of both the coated and the uncoated SiO_2 substrates were carried out in a 10 mM NaCl solution using an electrophoretic light-scattering spectrophotometer (ELS 8000, Otsuka Electron., Osaka, Japan) with a plate cell. Six measurements were applied to each sample.

2.6. Atomic force microscopy (AFM) analysis

AFM observations were performed with a commercial instrument (Bioscope, Nanoscope IIIa, Veeco, Santa Barbara, CA, USA). Images (1.0×1.0 μm^2 area) were acquired using the tapping mode of operation with a phosphorus (n) doped silicon cantilever (RTESP). The root-mean-square (rms) roughness was obtained to quantitatively describe the roughness of the surface topography. More than three measurements for each sample were recorded to calculate the average.

2.7. Measurement of static contact angle (SCA)

The static water contact angle of the surface was measured using an automatic contact angle meter (CA-W, Kyowa Interface Science, Saitama, Japan) at room temperature. At least six different areas were measured and averaged for each sample.

2.8. Measurement of dynamic contact angle (DCA)

DCA analyses were carried out using a Cahn DCA analytical instrument (model315, ATI, Madison, USA). Both coated and uncoated SiO_2 substrates with dimensions $30 \times 30 \times 0.5$ mm^3 were prepared for measurements. The substrates were lowered into ultrapure water at a speed of 80 μm s^{-1}. The software WindDCA (Cahn Instruments Inc.) was used to record and calculate the advancing contact angle (θ_A) and the receding contact angle (θ_R). Contact angle hysteresis is ($\theta_A - \theta_R$). The mobility factor (MF) of the surface was calculated by using the following equation: $MF = (\theta_A - \theta_R)/\theta_A$ [24].

2.9. Assessment of non-specific protein adsorption

The assessments were performed on both the coated and the uncoated SiO_2 substrates with a series of typical anionic and cationic proteins as aforementioned, according to a standard protocol as described by us elsewhere [25]. Simply, after equilibrated in water, the substrates (coated and uncoated) were immersed in 10 mL of protein solution (0.32 g L^{-1}, prepared in PBS buffer, pH 7.1), followed by an incubation at 37 °C for 1 h. Then the substrates were rinsed twice with sufficient PBS (pH 7.1) for 5 min each while stirring at 300 rpm. To detach all the adsorbed protein from the SiO_2 substrate, each substrate was immersed in 2.0 mL of 10 mg mL^{-1} sodium dodecyl sulfate (SDS) solution (water as solvent) in a small sealed case, followed by an ultrasonication for 10 min. The amount of protein in the SDS solution was determined by the Micro BCA (bicinchoninic acid) protocol (Micro BCA Protein Assay Kit, Pierce Biotechnology, Rockford, IL, USA).

2.10. Assessment of cell adhesion

The assessment of cell adhesion was carried out by using a mouse fibroblast cell line, L929 cells (RCB 0081, Cell Bank, Japan) as model cells. Both the coated and the uncoated SiO_2 substrates ($20 \times 20 \times 0.5$ mm^3) were placed in a 60 mm cell culture dish, and then 1 mL cell suspension (cell density: 1.0×10^5 cells mL^{-1}) in DMEM supplemented with 10% fetal bovine serum (FBS) was seeded on each substrate. After 2 h of incubation at 37 °C in a humidified atmosphere of 5% CO_2, 10 mL culture medium was added to the culture dish. Together with the substrates, the cells were cultured in the incubator. Before assessment, the substrates were rinsed with the medium to wash off the unattached cells. The cell adhesion was assessed by observing the substrates with a phase-contrast microscope (IX71S1F-2, Olympus, Tokyo, Japan).

3. Results and discussion

3.1. Molecular properties of cationic, neutral, and anionic MPC polymers

Fig. 1 shows the structures of the three MPC copolymers with or without charged moieties. Their molecular properties are listed in Table 1. Besides MPC, all three copolymers contain MPTMSi which is a typical methacrylate silane-coupling agent. Silane-coupling moieties such as the MPTMSi moieties in a copolymer are very useful in many biomedical applications because they can react with various inorganic materials such as glass, silica, silicone, and metals to form a chemical bond with surface or can induce a crosslinkable coating on various organic materials such as poly(ethylene terephthalate) (PET), poly(vinyl chloride) (PVC), etc. [26]. The compositions of MPTMSi in all three copolymers are higher than 10%, a composition which has been proved sufficient for an MPC copolymer to form a stable covalent coating on a SiO_2 substrate [11]. The MTAC moieties of PMBASi and the PMPS moieties of PMBSSi are two types of methacrylate units respectively having oppositely charged groups. A serial PMBASi copolymers containing varying compositions of MTAC were synthesized and characterized. In this study, the PMBASi containing 18% mole fraction of MTAC were chosen because it had an approximately equal absolute value of ζ-potential as the available PMBSSi had. Both PMBASi and PMBSSi have hydrophobic moieties, i.e. BMA, favoring us to elucidate the role of the hydrophobic moieties in the copolymer by comparing with the super hydrophilic PMSi which has no BMA moiety. Furthermore, PMBASi and PMBSSi share another common feature as they contain almost same amounts of the MPC fraction. As shown in Table 1, all these three MPC polymers have similar molecular weights, possess narrow polydispersities, and are soluble in both water and ethanol. These molecular characteristics make the three MPC copolymers comparable and fit for a comparative investigation as model copolymers.

3.2. Interfacial properties of coatings

3.2.1. Sample surfaces

The SiO_2 (quartz) substrate was used in the study in consideration of its high purity, clear chemical structure, well-defined silane reactivity, and most importantly, wide applications as various biomaterials. To characterize the interfacial properties of these copolymers, SiO_2 substrates respectively with three copolymer covalent coatings were prepared according to a same protocol as

described in section Materials and methods. Including uncoated, PMBASi-coated, PMSi-coated, and PMBSSi-coated SiO_2 substrates, four sample surfaces were used in the subsequent investigations. Fig. 2 illustrates the differences between the four sample surfaces with highlighting the variation in the surface charge.

3.2.2. X-ray photoelectron spectroscopy (XPS)

The sample surfaces were analyzed by XPS. Their spectra of nitrogen (N_{1s}), phosphorus (P_{2p}), and silicon (Si_{2p}) are shown in Fig. 3. The XPS data of atomic concentrations of different sample surfaces are listed in Table 2. Those three MPC copolymers coated substrates were compared with the uncoated substrates. XPS signals at 133 eV attributed to the phosphorus 2p peak and at 402 eV attributed to the nitrogen 1s peak were detected on the PMBASi-, PMSi-, and PMBSSi-coated substrates but not on the uncoated substrates (Fig. 3), revealing the existence of MPC moieties on these coated substrates. On both the PMBSSi- and the PMSi-coated surfaces, the atomic concentrations of nitrogen and phosphorus were almost same, while on the PMBASi-coated surface, the nitrogen concentration was quite higher than the phosphorus concentration due to the trimethylammonium groups of the MTAC moieties on PMBASi (Table 2). The sulfur 2p peak (BE ~ 168 eV) was only detected on the PMBSSi-coated surface, owing to the sulfonate groups of PMPS moieties on PMBSSi. Furthermore, signals at 102 eV attributed to the silicon 2p peak were detected on all samples regardless of whether or not polymer coatings were applied (Fig. 3). However, the atomic concentrations of silicon on the MPC copolymers coated substrates were greatly lower than those on the uncoated substrate (Table 2), suggesting that the substrates were effectively covered by the coating. These results indicate that the substrates were successfully modified by these MPC copolymers.

3.2.3. Surface ζ-potential

The coatings not only changed the surface elemental composition but also altered the surface charge of the original substrate. After coating, the charged moieties of the copolymer played their functions in the form of the interface. The surface ζ-potentials of sample surfaces were measured to characterize their surface charge in the aqueous environment. As shown in Fig. 4, after coated with the neutral MPC copolymer PMSi, the ζ-potential of the substrate changed from an original value of -47.4 ± 0.9 mV to a value of near 0 mV; the cationic PMBASi-coated substrates and the anionic PMBSSi-coated substrates exhibited ζ-potentials of 26.1 ± 0.6 mV and -24.2 ± 2.5 mV, respectively; the signs of the ζ-potential values were finely in agreement with the variation in the charge properties of the corresponding copolymers; the absolute values of two ζ-potentials of cationic PMBASi and anionic PMBSSi coatings were approximately equal, making them quite comparable. These features indicate that after coating, the charge of the original substrate was shielded, and as a result the polymer layer instead of the surface of the original substrate became to dominate the surface charge condition.

3.2.4. Atomic force microscopy (AFM) and surface roughness

The surface topographies before and after coating were characterized by AFM. The topography images (Fig. 5) demonstrate that all three coated surfaces exhibited as smooth as the uncoated surfaces. The smoothness of sample surfaces was quantitatively verified by analyzing their rms roughness. The uncoated substrate had a very low rms value of 0.43 ± 0.27 nm. The PMBASi-, PMSi-, and PMBASi-coated surface exhibited rms values of 0.36 ± 0.19 nm, 0.15 ± 0.03 nm, and 0.37 ± 0.14 nm, respectively. The rms roughness values of the three coated surfaces were approximate to or lower than that of the uncoated surface, indicating that these coatings did not induce the increase in the surface roughness. Especially, the cationic PMBASi and the anionic PMBSSi-coated surfaces had almost equal rms roughness values, suggesting the type of the charged moiety may not affect the surface roughness.

3.2.5. Surface wettability

To investigate the surface wettability, both the static contact angle (SCA) analysis and the dynamic contact angle (DCA) analysis were performed. The uncoated SiO_2 substrate was hydrophilic as it had a 31.2° static contact angle. When a PMSi coating was

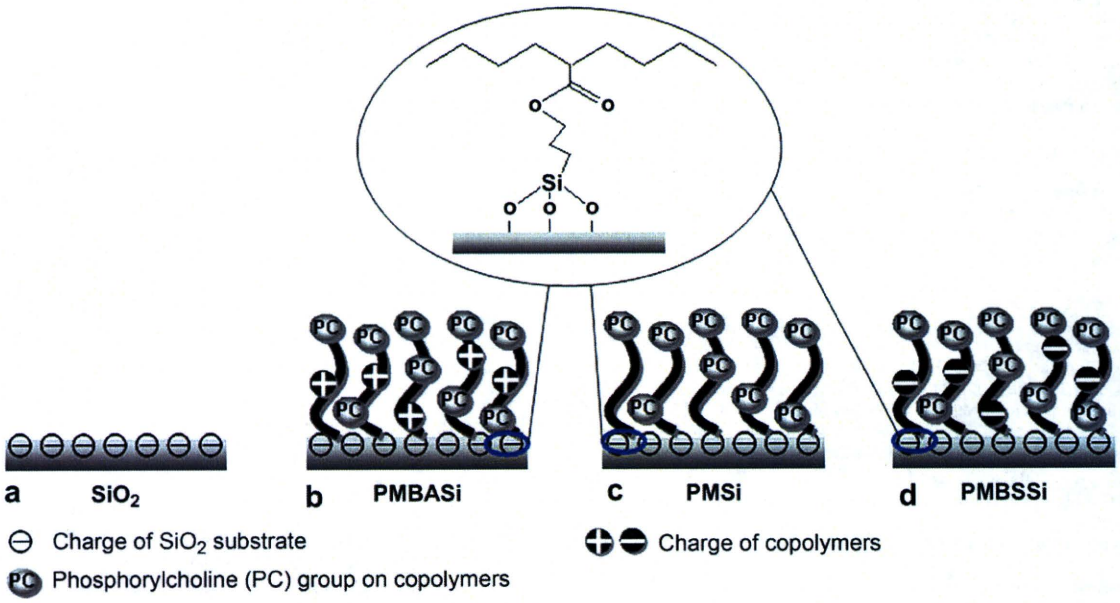

Fig. 2. Sample surfaces used in this study that are prepared using different MPC copolymers and exhibit different surface charges. (a) Uncoated SiO_2; (b) PMBASi-coated SiO_2; (c) PMSi-coated SiO_2; and (d) PMBSSi-coated SiO_2. The inset demonstrates the chemical bond between the SiO_2 substrate and the MPC polymers.

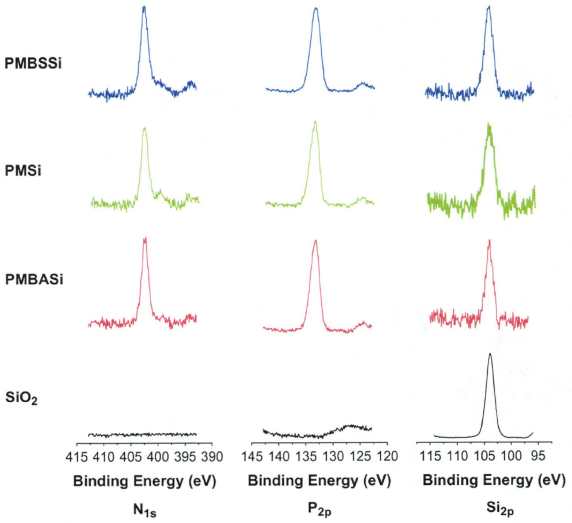

Fig. 3. XPS spectra of nitrogen (N_{1s}), phosphorus (P_{2p}), and silicon (Si_{2p}) on different sample surfaces.

applied, the average contact angle decreased to 10.5°, indicating a highly hydrophilic surface. Both static contact angles of the PMBASi- and the PMBSSi-coated surfaces were lower than that of the uncoated SiO_2 surface but higher than that of the PMSi-coated surface. This reveals that, on the one hand both the PMBSASi and the PMBSSi coatings were quite hydrophilic in general, and on the other hand the hydrophobic moieties (i.e., BMA) on both coatings were likely to affect the surface wettability. The role of BMA moieties in the surface wettability was further elucidated by the DCA analysis. The DCA measurement is an easy method to determine the advancing and receding contact angles which are parameters of the surface wettability. The advancing contact angle, θ_A, is sensitive to the hydrophobic surface component, and the receding contact angle, θ_R, is sensitive to the hydrophilic surface component. The DCA profile provides dynamic information on the process from a dry state to a wet state of a surface when in contact with an aqueous medium. Fig. 6 shows the DCA profiles of different sample surfaces. Table 3 summarizes the values of θ_A and θ_R obtained from Fig. 6. As shown in Table 3, in contrast to the PMSi-coated surface, which displayed a low θ_A and a supper low θ_R corresponding to a small hysteresis (Fig. 6), both the PMBASi- and the PMBSSi-coated surfaces had quite high θ_A and low θ_R, resulting in large hystereses (Fig. 6). Under dry conditions the phosphorylcholine groups of PMBASi and PMBSSi were covered with the hydrophobic moieties of polymer chains to minimize the surface free energy, while the hydrophilic moieties (especially phosphorylcholine groups) became to expose to the aqueous environment to reduce the interfacial energy when contact with water. Hence, the observed large hystereses of PMBASi and PMBSSi may be related to the reorientation of the phosphorylcholine groups when the surface changed from a dry state to a wet state. Through a surface reorientation process, the phosphorylcholine groups would become to dominate the

Table 2
Atomic concentrations of different sample surfaces determined by XPS measurements.

Sample surface	Atomic concentration (%)					
	C_{1s}	O_{1s}	N_{1s}	P_{2p}	S_{2p}	Si_{2p}
SiO_2	8.9	60.7	n.d.	n.d.	n.d.	30.4
PMBASi	62.8	28.1	4.5	3.2	n.d.	1.4
PMSi	60.1	28.7	4.8	4.8	n.d.	1.6
PMBSSi	61.9	28.9	3.7	3.8	0.5	1.2

n.d.: not detected.

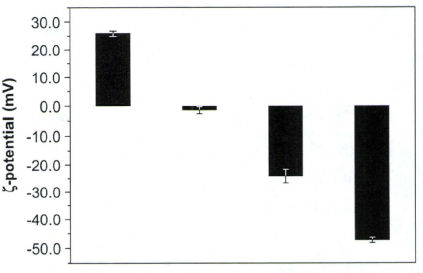

Fig. 4. Surface ζ-potentials of different sample surfaces. Data are mean ± SD, $n = 6$.

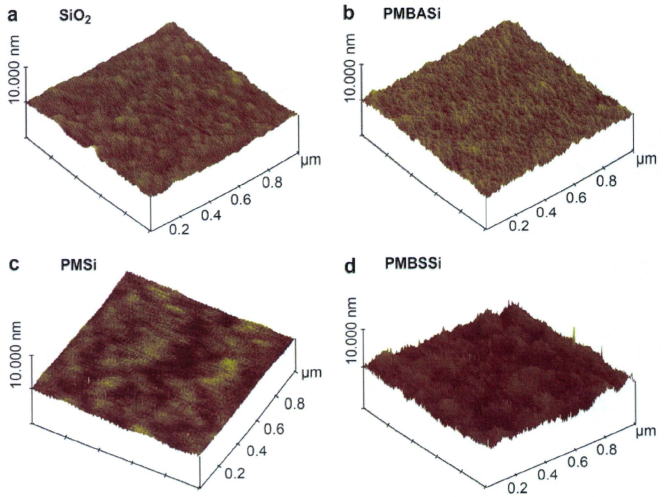

Fig. 5. AFM images (1.0 µm × 1.0 µm areas) of different sample surfaces. (a) Uncoated SiO_2; (b) PMBASi-coated SiO_2; (c) PMSi-coated SiO_2; and (d) PMBSSi-coated SiO_2.

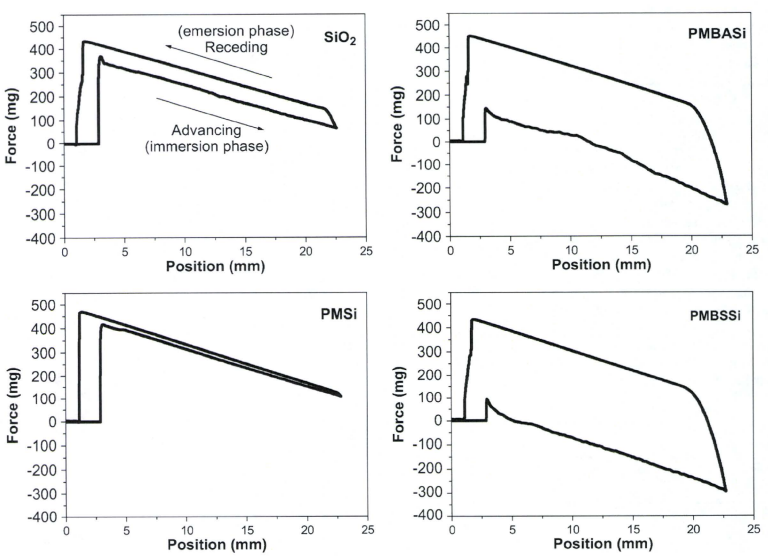

Fig. 6. DCA profiles of different sample surfaces being lowered into ultrapure water at a speed of 80 µm s^{-1}.

Table 3
Advancing and receding contact angles of different sample surfaces.

Sample surface	Contact angle (°)		Hysteresis	Mobility Factor
	Advancing	Receding		
SiO_2	37.1	19.3	17.8	0.48
PMBASi	72.0	11.3	60.7	0.84
PMSi	22.3	0.0	22.3	1.00
PMBSSi	84.4	15.9	68.5	0.81

outmost surface and thereby the hydrophobic moieties would be buried. This is believed very important for an MPC copolymer to play their functions in aqueous mediums [27,28]. According to the value of mobility factor (MF), both the PMBASi- and the PMBSSi-coated surfaces had high mobilities of the polymer chains, implying that when in contact with an aqueous environment, surface reorientation may easily occur in both PMBASi- and PMBSSi-coated surfaces. In addition, a very small hysteresis was observed in the DCA profile of the PMSi-coated surface, which is possibly because phosphorylcholine groups enriched the polymer network and abundantly existed at the surface even under dry conditions [24]. Therefore, the nature of the observed difference in the dynamic wetting process between the PMSi surface and the PMBASi or PMBSSi surface should be ascribed to the introduction of the BMA moieties, which contributed to the hydrophobic surface component and increased the surface hydrophobic/hydrohphlic heterogeneity in the coatings.

3.3. Protein adsorption

The sample surfaces were exposed to a group of proteins to investigate the effects of the surface charge and chemistry on protein adsorption. Based on the electrical nature, we chose pepsin ($pI = 1.0$) and BSA ($pI = 4.7$) as typical anionic proteins and ribonuclease A (RNase A, $pI = 9.5$) and lysozyme (LYZ, $pI = 11.0$) as typical cationic proteins, respectively. We chose a 1× PBS buffer with a medium ionic strength (about 137 mM) and pH (about 7.1), allowing a better simulation of the typical physiological condition used in various biological applications. Fig. 7 shows the adsorbed amounts of four proteins on uncoated, PMBASi-coated, PMSi-coated, and PMBSSi-coated SiO_2 substrates, determined with a microBCA protocol which is a widely used method to measure trace amount of protein in solution.

The surface coatings remarkably affected the adsorption of the proteins. All proteins, despite their different charge properties, seriously adsorbed to the uncoated SiO_2 substrate, exhibiting high adsorbed amounts. In contrast, the adsorbed protein amounts on three MPC copolymers coated surfaces were pronouncedly low in general. After coating, 82–98% reductions in protein adsorption were obtained in comparison with the corresponding behavior on the uncoated SiO_2 substrates. Generally, a surface with a ζ-potential of about 26.1 mV (ζ-potential of PMBASi) or −24.2 mV (ζ-potential of PMBSSi) can induce protein adsorption significantly. For example, Ikada et al. reported the amounts of BSA adsorption on the different charged monomer grafted

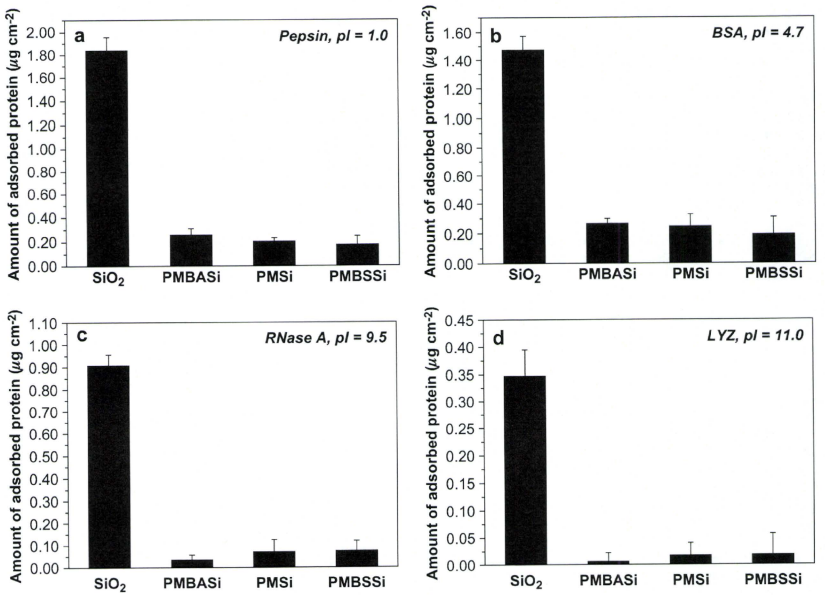

Fig. 7. Amounts of typical cationic proteins and anionic proteins adsorbed on different sample surfaces. (a) pepsin, $pI = 1.0$; (b) BSA, $pI = 4.7$; (c) RNase A, $pI = 9.5$; and (d) LYZ, $pI = 11.0$.

polyethylene (PE) film surfaces [19]. They carried out the protein adsorption experiments under a similar condition as we used in our experiments. Their results indicated that, the adsorbed amount of BSA on the acrylic acid (AA) grafted PE surface with a ζ-potential of −27.3 mV was 0.78 μg cm^{-2}, an amount which is much higher than that on the PMBSSi surface with a similar ζ-potential; and the adsorbed amount of BSA on the *N,N*-dimethylaminopropyl acrylamide (DMAPAA) grafted PE surface with a ζ-potential of 17.0 mV was 4.76 μg cm^{-2}, an amount which is significantly higher than that on the PMBASi surface with a higher ζ-potential of 26.1 mV. This comparison clearly reveals that despite the charged moieties involved, the MPC moieties on the copolymer still played their role effectively in suppression of protein adsorption. In addition, the adsorbed protein amounts on both the cationic PMBASi surface and the anionic PMBSSi surface were in a similar low level as those on the neutral PMSi surface, with no statistical difference significance. These results indicate that the incorporation of charged moieties would not significantly influence the protein resistant property of an MPC copolymer. Based on previous studies on the effects of ionic strength on protein adsorption, we have made a hypothesis that the function of MPC moieties in the suppression of protein adsorption, rather than the electrostatic character resulting from the charged moieties, dominated the interactions between the protein and the charged MPC copolymer surfaces [11]. The results of this study test, support, and expand the hypothesis.

Considering that the MPC mole fractions in both PMBASi and PMBSSi were only about half of that in PMSi, the fact of no big difference in the protein adsorption on the neutral PMSi surface in comparison with on the charged PMBASi or PMBSSi surfaces implies that, an about 50% mole fraction of the MPC moiety in a copolymer is sufficient to construct a protein adsorption resistant surface and additional more fraction seems not to bring more reduction in the protein adsorption. In addition, as the charged PMBASi and PMBSSi contain hydrophobic moieties (i.e. BMA) but the neutral PMSi dose not, the similar level of protein adsorption meanwhile suggests that the introduction of the hydrophobic moieties in an MPC copolymer surface may not result in an increase in the protein adsorption if the MPC moiety is predominant in the copolymer composition. This should be associated with the fact that both the PMBASi and the PMBSSi surfaces had high mobility as elucidated by the DCA analysis (Fig. 6 and Table 3). The high mobility facilitates the surface reorientation when the surface is in contact with an aqueous medium, and the hydrophobic components (for example, BMA in both PMBASi and PMBSSi) are buried in the inner of the polymer layer as the hydrophilic components such as MPC moieties migrate to the outmost surface to minimize the surface energy [27,28]. The MPC moieties are predominant at the surface and thereby dominate the surface properties, especially such as the interactions with proteins when in contact with a protein solution.

Although the adsorbed protein amounts on three coated surfaces had no statistical difference significance with each other, quantitatively they still present a subtle but systematic dependence on the surface charge. When ranking the amounts of protein adsorbed on the different coated surfaces, in the cases of negatively charged pepsin and BSA (Fig. 7a and b), the order is PMBASi (cationic) > PMSi (neutral) > PMBSSi (anionic), while in the cases of positively charged RNase A and LYZ (Fig. 7c and d), the order is PMBASi (cationic) < PMSi (neutral) < PMBSSi (anionic). This can be correlated to the possible electrostatic interactions between the charged proteins and the charged surfaces [17]. However, as discussed above, the possible effect from electrostatic interactions would be too small and too limited to influence the overall situation.

3.4. Cell adhesion

At the molecular level, it is generally believed that the rapid adsorption of proteins to the surface is the initial stage of cell adhesion [29]. In view of the high capability of the three MPC copolymers to suppress protein adsorption, we supposed that they would have corresponding capability to resist the cell adhesion. Mouse fibroblast L929 cells, which are typical adherent cells and are widely used in various biological studies and evaluations as model cells, were employed to evaluate the cell adhesion on the sample surfaces. Fig. 8 shows the microscopic images of sample surfaces on which L929 cells were cultured for one day and four days. In the case of uncoated surface, L929 cells gradually adhered,

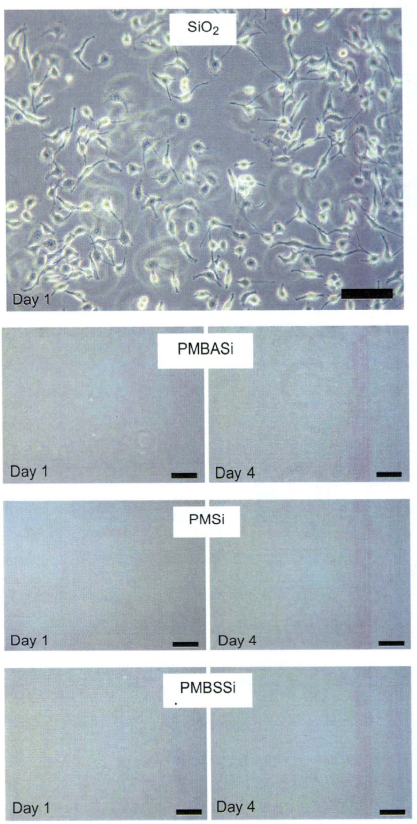

Fig. 8. Microscopic images of different sample surfaces on which L929 cells were cultured for one day and four days. MPC copolymers coated SiO_2 surfaces exhibited no cell adhesion, while uncoated SiO_2 exhibited serious cell adhesion. Scale bar represents 100 μm.

spread, and flattened on the surface after seeded, and then formed confluence after cultured for one day (Fig. 8), and finally densely covered the surface four days later (data not shown). In contrast, no cell adhesion was observed on PMBASi, PMSi, and PMBSSi surfaces after cultured for one day and even for four days (Fig. 8). This indicates that like the neutral PMSi, both the cationic PMBASi and the anionic PMBSSi possess the high capability to suppress cell adhesion due to the MPC moieties at the surface. Ikada et al. reported that cells could adhere and proliferate on the charged monomer grafted PE surfaces with a ζ-potential larger than 12 mV [19]. Before we performed the evaluation, we had previously speculated that the cationic PMBASi surface might induce cell adhesion because of the possibly increased electrostatic attraction between the positive charged surface of the coating and the negatively charged surface of the cell. Evidently, the evaluation result overturned the speculation, and it seems that the charged moieties in PMBASi and PMBSSi would not cause the effect in inducing cell adhesion. This further supports our aforementioned hypothesis that the electrostatic character resulting from the charged moieties of the copolymers would not dominate the surface behaviors of bioadsorptions.

4. Conclusions

The behaviors of protein adsorption and cell adhesion on three model MPC copolymer surfaces with different surface charges were comparatively investigated. Results imply that the introduction of charged moieties, either the cationic or the anionic, in an MPC copolymer, would not increase the risk in inducing both the protein adsorption and cell adhesion. This tests, supports, and expands our previous hypothesis that the function of MPC moieties in the suppression of protein adsorption, rather than the electrostatic character resulting from the charged moieties, would dominate the interactions between proteins/cells and MPC copolymer surfaces. These electrically charged MPC copolymer surfaces can be applied to those biological applications simultaneously requiring non-biofouling properties and electrical properties.

Acknowledgement

This work was supported by Grant-in-Aid for Scientific Research on Innovative Areas "Molecular Soft-Interface Science" from the Ministry of Education, Culture, Sports, Science and Technology of Japan.

Appendix

Figures with essential colour discrimination. Certain figures in this article, in particular Figures 2, 3, 5 and 8, are difficult to interpret in black and white. The full colour images can be found in the on-line version, at doi:10.1016/j.biomaterials.2009.06.005.

References

[1] Ishihara K, Ueda T, Nakabayashi N. Preparation of phospholipid polymers and their properties as polymer hydrogel membranes. Polym J 1990;22:355–60.
[2] Ishihara K, Nomura H, Mihara T, Kurita K, Iwasaki Y, Nakabayashi N. Why do phospholipid polymers reduce protein adsorption? J Biomed Mater Res 1998;39:323–30.
[3] Iwasaki Y, Ishihara K. Phosphorylcholine-containing polymers for biomedical applications. Anal Bioanal Chem 2005;381:534–46.
[4] Palmer RR, Lewis AL, Kirkwood LC, Rose SF, Lloyd AW, Vick TA, et al. Biological evaluation and drug delivery application of cationically modified phospholipid polymers. Biomaterials 2004;25:4785–96.
[5] Chim YTA, Lam JKW, Ma Y, Armes SP, Lewis AL, Roberts CJ, et al. Structural study of DNA condensation induced by novel phosphorylcholine-based copolymers for gene delivery and relevance to DNA protection. Langmiur 2005;21:3591–8.
[6] Chiba N, Ueda M, Shimada T, Jinno H, Watanabe J, Ishihara K, et al. Development of gene vectors for pinpoint targeting to human hepatocytes by cationically modified polymer complexes. Eur Surg Res 2007;39:23–32.
[7] Zhao XB, Pan F, Coffey P, Lu HR. Cationic copolymer-mediated DNA immobilization: interfacial structure and composition as determined by ellipsometry, dual polarization interferometry, and neutron reflection. Langmuir 2008; 24:6881–8.
[8] Morille M, Passirani C, Vonarbourg A, Clavreul A, Benoit JP. Progress in developing cationic vectors for non-viral systemic gene therapy against cancer. Biomaterials 2008;29:3477–96.
[9] Allen TM, Cullis PR. Drug delivery systems: entering the mainstream. Science 2004;303:1818–22.
[10] Xu Y, Takai M, Konno T, Ishihara K. Microfluidic flow control on charged phospholipid polymer interface. Lab Chip 2007;7:199–206.
[11] Xu Y, Takai M, Ishihara K. Suppression of protein adsorption on a charged phospholipid polymer interface. Biomacromolecules 2009;10:267–74.
[12] Ge XW, Ye Q, Xu XL, Zhang ZC, Chu GS. Studies of inverse emulsion copolymerization of (2-methacryloyloxyethyl) trimethyl ammonium chloride and acrylamide. J Appl Polym Sci 1998;67:1005–10.
[13] Hou SJ, Ha RH. The electrochemical analysis of cationic water soluble polymer. Eur Polym J 1998;34:283–6.
[14] Roach P, Farrar D, Perry CC. Surface tailoring for controlled protein adsorption: effect of topography at the nanometer scale and chemistry. J Am Chem Soc 2006;128:3939–45.
[15] Mrksich M. A surface chemistry approach to studying cell adhesion. Chem Soc Rev 2000;29:267–74.
[16] Ostuni E, Yan L, Whitesides GM. The interaction of proteins and cells with self-assembled monolayers of alkanethiolates on gold and silver. Colloid Surf B Biointerfaces 1999;15:3–30.
[17] Pasche S, Voros J, Griesser HJ, Spencer ND, Textor M. Effects of ionic strength and surface charge on protein adsorption at PEGylated surfaces. J Phys Chem B 2005;109:17545–52.
[18] Ladd J, Zhang Z, Chen S, Hower JC, Jiang S. Zwitterionic polymers exhibiting high resistance to nonspecific protein adsorption from human serum and plasma. Biomacromolecules 2008;9:1357–61.
[19] Kishida A, Iwata H, Tamada Y, Ikada Y. Cell behavior on polymer surfaces grafted with nonionic and ionic monomers. Biomaterials 1991;12:786–92.
[20] Rechendorff K, Hovgaard MB, Foss M, Zhdanov VP, Besenbacher F. Enhancement of protein adsorption induced by surface roughness. Langmuir 2006;22:10855–88.
[21] Anselme K, Bigerelle M, Noel B, Dufresne E, Judas D, Iost A, et al. Qualitative and quantitative study of human osteoblast adhesion on materials with various surface roughnesses. J Biomed Mater Res 2000;49:155–66.
[22] Sethuraman A, Han M, Kane RS, Belfort G. Effect of surface wettability on the adhesion of proteins. Langmuir 2004;20:7779–88.
[23] Arima Y, Iwata H. Effect of wettability and surface functional groups on protein adsorption and cell adhesion using well-defined mixed self-assembled monolayers. Biomaterial 2007;28:3074–82.
[24] Futamura K, Matsuno R, Konno T, Takai M, Ishihara K. Rapid development of hydrophilicity and protein adsorption resistance by polymer surfaces bearing phosphorylcholine and naphthalene groups. Langmuir 2008;24:10340–4.
[25] Jang K, Sato K, Mawatari K, Konno T, Ishihara K, Kitamori T. Surface modification by 2-methacryloyloxyethyl phosphorylcholine coupled to a photolabile linker for cell micropatterning. Biomaterials 2009;30:1413–20.
[26] Lewis AL, Cumming ZL, Goreish HH, Kirkwood LC, Tolhurst LA, Stratford PW. Crosslinkable coatings from phosphorylcholine-based polymers. Biomaterials 2001;22:99–111.
[27] Clarke S, Davies MC, Roberts CJ, Tendler SJB, Williams PM, O'Byrne V, et al. Surface mobility of 2-methacryloyloxyethyl phosphorylcholine-co-lauryl methacrylate polymers. Langmuir 2009;16:5116–22.
[28] Feng W, Zhu SP, Ishihara K, Brash JL. Adsorption of fibrinogen and lysozyme on silicon grafted with poly(2-methacryloyloxyethyl phosphorylcholine) via surface-initiated atom transfer radical polymerization. Langmuir 2005; 21:5980–7.
[29] Ostuni E, Chapman RG, Liang MN, Meluleni G, Pier G, Ingber DE, et al. Self-assembled monolayers that resist the adsorption of proteins and the adhesion of bacterial and mammalian cells. Langmuir 2001;17:6336–43.